Astron. Astrophys. 363, 455–475 (2000)

ASTRONOMY AND ASTROPHYSICS

Wind-type outflows in Seyfert 1 active nuclei

P. Pietrini and G. Torricelli-Ciamponi

[1] Dipartimento di Astronomia e Scienza dello Spazio, Università di Firenze, Largo E. Fermi 5, 50125 Firenze, Italy
[2] Osservatorio Astrofisico di Arcetri, Largo E. Fermi 5, 50125 Firenze, Italy

Received 8 December 1999 / Accepted 16 August 2000

Abstract. A sub-relativistic, thermal wind-type flow could represent the physical connection between the central engine and other observed components of the central region, such as the Broad Line Region (BLR) and X-ray/UV absorbers.

Observational clues as to the existence of such outflows in radio-quiet Active Galactic Nuclei (AGNs) are provided, for instance, by blue shifted absorption lines in Seyferts and Broad Absorption Line Quasi Stellar Objects (BAL QSOs).

We study a model for wind-type flows in Seyfert 1s and explore the physical conditions of the outflowing gas, taking into account explicitly both heating and cooling processes, including Compton interaction with radiation. A distributed heating source along the wind way turns out to be necessary for this nuclear wind existence and restrictions on physical parameters to obtain a reasonable wind model in the AGN context are identified; we also allow for externally originated mass loading of the wind.

Key words: hydrodynamics – plasmas – radiation mechanisms: thermal – galaxies: active – galaxies: Seyfert

1. Introduction

Basic ingredients of the AGN complex phenomenology are universally accepted to be a central supermassive black hole and mass accretion on it. In fact, another component seems to be a general property of the physics of these objects, that is the existence of mass and energy outflows from the central region (Laing 1996, Blandford 1993, Ulrich 1988). They appear as strongly collimated, high velocity (even relativistic in many cases) jets in radio-loud objects, where they can represent the most important element both from the observational point of view and for what regards the theoretical explanation of the nuclear activity (Blandford 1994, Zensus 1996, Laing 1996), typically with non-thermal mechanisms dominating. On the other hand, radio-quiet AGNs also show clear indications for the presence of generally sub-relativistic outflows from the central zone (Ulrich 1988, Stocke et al. 1994, Crenshaw et al. 1999, Turnshek 1988, Turnshek 1995, Weymann et al. 1997), both for Seyfert 1 objects, and for more luminous and distant QSOs. In particular, UV observations, from the International Ultraviolet Explorer (IUE) (Ulrich 1988), the Hopkins Ultraviolet Telescope (HUT) and, in the last years, the Hubble Space Telescope (HST), have shown the presence of UV absorption lines blue-shifted with respect to the corresponding broad emission lines, in the spectra of a number of Seyfert 1s, indicating outflow of the absorbing gas (Crenshaw et al. 1999). This looks like the analogue of the much more remarkable and observationally well known phenomenon of broad absorption lines observed in 10–15% of QSOs (BAL QSOs), characterized by a conspicuous blue-shift with respect to the emission lines, implying much larger outflow velocity (Weymann et al. 1997, Stocke et al. 1994, Turnshek 1995). Indeed, UV absorbers seem to be a more general property of lower luminosity objects, such as Seyfert 1s, since blue-shifted UV absorption features are observed in $\sim 50 \div 70\%$ of the AGNs of this class. Also, recent work (Crenshaw et al. 1999) suggests that, at least for Seyfert nuclei, there is a one-to-one correspondence between the objects that show intrinsic UV-absorption from outflowing material and X-ray "warm absorbers", thus showing that these two phenomena could be correlated. There have been suggestions and attempts to relate UV and X-ray absorbers, possibly identifying them with a single component of the AGN structure (see for example Mathur 1997; Mathur et al. 1995; Mathur et al. 1997). Although we could still reasonably imagine a connection between UV and X-ray absorption, recent observations have shown that, with high spectral resolution, multiple velocity components appear in UV absorption (Mathur et al. 1999; Crenshaw et al. 1999), thus indicating that the physical picture of AGN absorbers may be more complicated and the search for the identification of a single absorbing structural component can be an oversimplification of the real structure (George et al. 1998).

UV absorbers are in general modeled with outflowing clumpy material embedded in a background medium, whose relationship with the absorbing clumps is not yet unequivocally determined. We refer to de Kool (1997) for a review of dynamical models of UV absorbing gas and the problems to be solved in both Seyferts and QSOs. Indeed, a series of physical reasons requires the clumpy UV absorbing material to be basically comoving with a surrounding medium, although it is a matter of debate whether the absorbers can be thermally confined by this background outflow and what is the origin of the clumps (instabilities developing in the background wind or injected and

dragged along clouds). It is not our present aim to model the details of the relationship between the UV absorbing material and the surrounding medium, however the presence of these outflowing absorbers in radio-quiet AGNs, together with the physical necessity that they are comoving with ambient material, is an indication for the existence of global outflows in these AGN classes, and it motivates our present research for a better understanding of the possible physical structure and characteristics of a global outflow, presumably originating in the very central regions and expanding out to large distances as a kind of background/connection for the various more observationally noticeable components of the AGN structure. This wind could have an important role in defining a physical connection underlying the various components of the AGN structure that can be identified by interpreting observations.

To this regard, it will be necessary to account for the relation of the wind with another phenomenologically quite distinctive component of AGNs, namely the BLR, whose modeling also is a matter of debate; in fact, the presence of a wind-type outflow as a surrounding medium for the broad line region cloud-like structures can have an influence on their physical modeling, as we briefly outline in the following. Two scenarios that could be explored are the following: a) BLR interpreted like a region in which a large number of small clouds emits the observed lines, broadened by the cloud motions; these clouds could be continuously created by the development of local condensations in a thermal-type instability of the wind, localized in the region of interest; b) broad lines emitted by winds or expanding envelopes of giant stars ("bloated star" model, see Alexander & Netzer 1994): in this case, the interaction between the AGN wind from the central region and the expanding envelopes must be analysed. This topic will be treated extensively in a forthcoming paper, whereas here we just briefly mention the main issues. Recent observational work (see Wandel et al. 1999 and references therein) as shown that broad line emitting cloud-like structures should be preferentially characterized by keplerian motion, so that the interaction of such motions with the surrounding wind gas must be studied. Indeed, if the background medium is outflowing and the "clouds" have keplerian motions, a "drag force problem" does exist (Korista 1999, Mathews & Ferland 1987) and the "clouds" must be somehow continuously replenished: this would point to the choice of a "bloated star"-like scenario for BLR modeling. As a consequence, the analysis of nuclear outflows can help to define some limitations to BLR models.

Moreover, within the accepted scenario for AGN description, in which an accretion disk is thought to be feeding the central black hole, the existence of a hot, tenuous "corona" around the central part of the disk is expected, as an effect of dissipation of accretion energy in the rarefied, "peripheral" regions, more distant from the equatorial plane of the disk itself. The hot coronal gas is believed to be substantially responsible for the X-ray emission from these AGNs reproducing the main properties of the observed hard-X-ray continuum (see, for example, Haardt & Maraschi 1993, Haardt et al. 1994). The specific physics of this coronal region is not very well established. However, allowing for a sort of analogy with the solar corona, the existence of a hot plasma wind, possibly emerging from the coronal region itself, seems to be justified from a theoretical point of view as well (see Liang & Price 1977); in fact, within this framework, some of the coronal plasma could be accelerated in a hot wind-type flow or, still within the analogy with solar-stellar coronae, the origin of wind-type outflowing gas could be expected to be related to the expansion of part of the hot coronal gas, as first suggested for accretion disk coronae by Liang & Price (1977).

Our specific aim in the present paper is then to investigate and identify the physical hypotheses and conditions that allow a wind-type solution to exist, by solving the appropriate hydrodynamical equations in which we take into account the heating and cooling processes relevant to the problem, and include Compton interaction of the wind plasma with the ionizing UV-X-ray radiation field centrally generated; we look for an outflow solution whose physical properties are "acceptable" within the general AGN scenario and range of expected physical parameters for plasma in Active Nuclei.

Various authors have already analyzed some aspects of wind-type outflows in AGNs, but in general referring to very specific regions or distance scales; Weymann et al. (1982) have proposed a hot plasma wind aiming to confine BLR clouds, but they were interested in radii $\gtrsim 10^{17}$ cm, and also they did not take Compton interactions into account directly. Raine & O'Reilly (1993) also discussed a hydrodynamic wind model, but, again they did not take into account the regions closer to the central black hole. Several other models have been put forward in the last years, trying to connect with the BLR (see for example the magnetically supported model of Emmering et al. (1992) or Chiang & Murray 1996) or the BAL region (Murray et al. 1995). Also, recently some authors have started working on solutions envisaging both an advection-dominated disk-like inflow and an associated outflow, carrying away mass, angular momentum, and energy (see Blandford & Begelman 1999).

Indeed, the AGN context offers quite a complex situation to be studied, and in general special limits have been studied. It is our present purpose to try to solve the wind problem for the specific physical environment of the central region of a radio quiet AGN, accounting for the known physical mechanisms at work in a simplified but as complete as possible way. This also implies that we have to study this wind-type outflow on a very extended range of distances from the central black hole, which can be rather difficult in principle.

As a matter of fact, we restrict our attention to a range of luminosities identifying typical Seyfert 1 parameters, so that we look for a model wind endowed with terminal velocities $v << c$, typically $\lesssim 10^3\,\mathrm{km\,s^{-1}}$, as it is inferred from blueshifted UV absorption lines observed in Seyferts (Mathur et al. 1995, Mathur et al. 1997, Crenshaw & Kraemer 1999, Crenshaw et al. 1999), and we are not trying at present to specifically model BAL QSOs outflows, that can be much faster.

Finally, we would like to stress that the aim of the present work is essentially to construct a consistent hydrodynamical model for a basic outflow that can in principle be applied to the AGN context and can represent a kind of physical connec-

tion for the various phenomenological components of the AGN structure, identified from the observations. We defer a detailed exploration and analysis of the relation with these other components of the AGN to forthcoming papers.

The outline of the paper is the following. We summarize the characteristics we require to be fulfilled for the wind to be both physically consistent and viable to describe a global outflow in the central regions of radio-quiet AGNs in Sect. 2. The basic hydrodynamical equations governing the outflow are given in Sect. 3. Sect. 4 is devoted to the detailed description of the various heating and cooling terms we account for in the energy balance equation. We collect in Sect. 5 some qualitative considerations on AGN winds, and in Sect. 6 the problem is set in the form of wind equations and critical point definition. Since relativistic corrections can be significant for the energy equation of a sub-relativistically outflowing thermal plasma so hot that electron temperatures in its internal region can be trans-relativistic or definitely relativistic, such corrections are taken into account and described in Sect. 7. In Sect. 8 we summarize the results of our computations and the properties of our model wind-type outflow, both for models characterized by constant mass flux and for mass entraining winds; finally, Sect. 9 is devoted to the discussion of these properties and a few considerations and physical speculations referring to the specific AGN context, namely to the relation between the wind and the BLR and the wind and the UV absorbers, to be more extensively studied in future work.

2. AGN wind properties

In this section we explicitly describe and discuss the main assumptions, approximations and requirements we want a wind-type flow to fulfill to be descriptive, even though schematically, of our astrophysical problem.

As for the geometry of the wind, we might expect a wind that does not cover the whole 4π solid angle, at least not on every scale of distance (for example in the region in which an "obscuring" torus is present, we can imagine the wind surviving only in the "open" solid angle region, thus acquiring a cone-like geometry). However, as for symmetry properties, it is reasonable to simplify the wind description by assuming a spherical geometry and symmetry in any case, thus implying that all the relevant physical quantities only depend on the radial coordinate r, identifying the distance from the central black hole, and that the wind velocity is essentially radial.

There are some general properties and requisites that we ask to be verified for a wind-type outflow in an Active Galactic Nucleus to be modeled in a simple way.

1) The wind gas must be such that its total optical depth to photon scattering is $\tau_T < 1$: this is a necessary condition so as not to have to account for modifications in the spectrum and energy content of the central radiation field (illuminating the wind plasma) through Compton thick interactions; also, and substantially in other words, the power exchanged through Compton interaction must be negligible with respect to the total luminosity of the radiation field, so that we can neglect any significant effect on the central radiation field itself due to Compton interactions along the wind flow.

In fact, what we assume is that the radiation field that illuminates the wind is basically unchanged, along the wind and emerging from the nuclear region, by the presence of the wind itself, neither because of its interaction with the plasma electrons, nor because of the hot wind plasma emission by bremsstrahlung, that, consistently, turns out to be negligible with respect to the central source luminosity.

The issue above refer to requests that are due not only to our choice of a schematic treatment of the problem, but also rely on the idea that substantial contribution to the high energy radiation field preferentially comes from the inner region of the AGN. Moreover, we stress that these requirements refer to the tenuous wind as a background medium, and not to the denser phenomenological components identified as BLR and outflowing UV absorbers.

2) The flow velocity must be in sub-relativistic regime ($v/c \ll 1$), since we are referring to radio-quiet AGNs (Seyfert 1s), in which no extreme phenomenology, suggestive of relativistic flows, is observed.

3) We expect the wind total mass flux, $\dot{M}_{\rm w}$, to be much lower than the critical (Eddington) accretion rate, $\dot{M}_{\rm E} \equiv L_{\rm Edd}/(\eta c^2)$ [where η is the black hole accretion efficiency and it is $\eta \sim 0.1$ (Krolik 1999)], for a given central black hole mass: $\dot{M}_{\rm w} \ll \dot{M}_{\rm E}$. Actually $\dot{M}_{\rm w}$ should be $\lesssim \dot{M}_{\rm accr}$, the accretion mass flux, and, therefore, we can reasonably suppose it to be much lower than the critical value of the accretion mass flux itself.

The requirements above both characterize AGN environment and guarantee the consistency of the chosen treatment and astrophysical description of the AGN wind problem; on the other hand, their fulfillment ends up to strongly characterize the outcoming model wind as a hot and very tenuous one, especially in the external regions, as it will be discussed in the following sections.

We also have to require that the wind solutions we obtain show a "regular" behaviour all along the range of distances involved, *i.e.*, that the various physical quantities turn out to be non-diverging, so as to properly represent a physical solution for the outflow. In fact, diverging physical quantities would imply that the chosen starting hypotheses do not lead to a physical condition existing in nature for the AGN wind; on the contrary, if a range of parameters is found, corresponding to which a regular solution is obtained, the assumed framework can be analysed as possibly representative of the physics of the AGN wind.

Especially important is then the identification and the detailed treatment of relevant radiative losses, and of energy deposition and loss mechanisms for the wind plasma, including the interaction of the plasma itself with the central source radiation field, through Compton processes. Thus, heating sources for the thermal wind plasma and their radial distance dependence have to be included in the wind description. Our present choice is to account for the known sources of heating and momentum deposition, and of cooling mechanisms with a physically consistent

description and, on the other hand, to try to suitably parameterize an additional heating function contribution, so as to obtain a physically reasonable solution for the wind equations (see Sect. 4).

3. Hydrodynamical equations for a wind-type flow

We are dealing with a wind-type outflow, implying that we are assuming stationarity of the flow as a physically reasonable approximation; this may be effectively realized since the dynamical crossing time of the wind region we are interested in (that can be estimated as $\sim R/v \sim R/c_{\rm s}$, being R the length scale for the region and v the order of magnitude of the flow velocity, that is approximately the sound speed, $c_{\rm s}$) is always significantly shorter than any reasonable estimate of the duration of the active phase of the AGN galaxy (see Krolik & Vrtilek 1984).

The description we choose for the problem is a purely hydrodynamical one, thus totally neglecting any magnetic field dynamical influence. Also, as mentioned in Sect. 2, we assume that the wind is basically radial, and it can be described in spherical symmetry, that is, if g is the generic scalar physical quantity, we have $\partial g/\partial\phi = \partial g/\partial\theta = 0$. Moreover, since the relevant force terms in momentum equation are radial (pressure gradient, gravitational force, radiation force due to the radiation field of the central, point-like considered, source), the outflow velocity turns out to be purely radial ($v_r \equiv v$).

The starting equations are thus the usual stationary hydrodynamical equations:

$$r^2\rho v = A(r), \tag{1}$$

$$\rho v\frac{dv}{dr} = -\frac{dp}{dr} - \rho\frac{GM_{\rm BH}}{r^2} + \frac{H_{\rm tot}}{c} - v\frac{A'}{r^2} \tag{2}$$

$$\begin{aligned}\rho^\gamma\frac{v}{\gamma-1}\frac{d}{dr}\left(\frac{p}{\rho^\gamma}\right) &= -\frac{\rho^2}{m_{\rm H}^2}\Lambda(T) + H_*(1-v/c)\\ &\quad + H_{\rm Comp} - L_{\rm Comp} +\\ &\quad \frac{A'}{r^2}\left(\frac{v^2}{2} - \frac{\gamma}{(\gamma-1)}\frac{p}{\rho}\right),\end{aligned} \tag{3}$$

together with

$$p = \frac{\rho kT}{m_{\rm H}\mu}. \tag{4}$$

In the following we define explicitly the notations used and we describe the meaning of the various terms appearing in the equations.

Eq. (1) is the steady state continuity equation, generically written so as to allow for the possibility of inclusion of mass sources along the wind; $A(r)$ is a mass flux per steradiant, and can be expressed as $A(r) = A_0 f_{\rm m}(r)$, with A_0 a dimensional constant and the non-dimensional function $f_{\rm m}(r)$ that takes into account the dependence of the mass flux on radial distance from the central black hole, thus allowing for a mass source along the wind. In the simple case of no mass sources along the wind, *i.e.*, constant mass flux for the outflow, we have $f_{\rm m}(r) = const. = 1$. Also, we have defined

$$A' = A'(r) \equiv \frac{dA}{dr},$$

so that

$$\nabla\cdot(\rho\mathbf{v}) = (1/r^2)d(r^2\rho v)/dr = A'/r^2.$$

Of course, when the mass flux is constant, and there are thus no mass sources in the wind, we have $A' = 0$ and all the terms multiplied by A' in momentum equation and energy equation disappear. On the contrary, those terms are intrinsic to the derivation of hydrodynamic equations in case there is mass input in the wind (Bittencourt 1988). For an analogous formulation see also David et al. 1987; notice, however, that, differently from this last work, in our treatment we do not account explicitly for energy gain-loss to the wind due to the input of mass in the wind itself, since at this level we have no specific information about the thermal properties of the input material; instead, we suppose that possible energy exchanges due to mass loading of the wind can be implicitly accounted for by a parameterized heating rate H_* that is discussed in the following, in Sect. 4.4.

In momentum equation (2), $M_{\rm BH}$ is the mass of the central black hole, and

$$\frac{H_{\rm tot}}{c} = \frac{\rho\sigma_{\rm T}}{m_{\rm p}}\frac{F_{\rm rad}}{c} + H_*/c \tag{5}$$

represents the total momentum deposition rate, that we have written in a general form as the sum of two distinct contributing terms. The first term on the right hand side represents radiation pressure effects, that is radiation force density (force per unit volume) $f_{\rm rad} \equiv \rho\sigma_{\rm T}F_{\rm rad}/(m_{\rm p}c)$, where $F_{\rm rad}$ in our problem is the radial and only non-vanishing component of the radiation flux vector $\mathbf{F}_{\rm rad}$. In our approximation, it is simply $F_{\rm rad}/c = P_{\rm rad} = L_0/(4\pi r^2 c)$; in the following, we write $f_{\rm rad}$ with a notation similar to the other possible momentum deposition term, defining

$$H_{\rm rad} \equiv \frac{\rho\sigma_{\rm T}F_{\rm rad}}{m_{\rm p}},$$

which has the same physical dimensions as an energy exchange rate per unit volume, so that in general we can write

$$H_{\rm tot}/c = (H_{\rm rad} + H_*)/c. \tag{6}$$

We allow for a second momentum deposition term (H_*/c) representing the possible contribution due to the fraction of energy gain that goes directly into bulk kinetic energy, when the energy deposition rate H_* (dimensionally energy per unit time per unit volume and explicitly described in the following section) comes from a heating mechanism due to the interaction of the wind thermal plasma with a population of radially directed relativistic particles injected in the wind at its base, in principle similarly to the case examined in Weymann et al. 1982 (see also Begelman et al. 1991). We have formally taken into account this contribution to allow for the possibility of such an energy deposition mechanism and in that case, the actual energy deposition rate is $H_*(1-v/c)$, as it appears in our energy equation [Eq. (3)]. Indeed, this can be considered as a limit situation, but other physical mechanisms depositing heat are to some degree likely to transfer some momentum to the flow (see

Esser at al. 1997), although possibly less efficiently and with a more complex relation between the energy deposition rate and the corresponding momentum deposition rate. The other limit condition is that in which no momentum deposition is associated with the heating process, and in that case the second term in momentum deposition rate [Eq. (5) or (6)] vanishes and the factor $(1 - v/c)$, multiplying H_* in Eq. (3), reduces to unity. In the following, we build up models corresponding to the two limit conditions identified above.

Eq. (4) is the equation of state for the wind gas, that we suppose a pure $\gamma = 5/3$ hydrogen gas; in general, for the typical solutions we obtain, the temperature turns out to be quite high, so that the gas is essentially completely ionized, and we can safely assume $\mu = 1/2$.

4. Energy equation terms

We now describe the meaning and origin of the energy gain and loss terms appearing on the right side of the energy Eq. (3).

It is interesting to notice that, apart from the radiative cooling rate $\frac{\rho^2}{m_{\rm H}^2}\Lambda(T) = n^2\Lambda(T)$ (where n is the wind number density), all the other energy exchange rates (Compton cooling rate $L_{\rm Comp}$ included) have a somehow similar structure, of the type

$$\mathcal{H}(r) = \frac{\rho(r)}{r^2}\mathcal{F}(r), \tag{7}$$

where $\mathcal{H}(r)$ is the generic energy exchange rate per unit volume appearing in the hydrodynamic equations, and $\mathcal{F}(r)$ is a function characteristic of the rate we are referring to, depending on the radial distance and possibly on the temperature of the wind gas.

4.1. Possible interaction of thermal wind plasma with a relativistic electron population

We briefly discuss this possibility, since we had originally considered the plausibility of the contribution to the heating of the thermal wind plasma due to collisional (Coulomb-like or even due to collective effects) interaction with a population of non-thermal relativistic electrons, injected at the base of the wind into the thermal plasma. This non-thermal particle component could be reasonably supposed to be generated in the high energy processes close to the black hole and one possible speculation about their origin in the present context could have been related to magnetic reconnection processes in the magnetically active regions of the AGN coronal structure (see Birk et al. 1999 and references therein).

Indeed, other authors dealing with AGN winds (Weymann et al. 1982) or in any case with AGN hot thermal diffuse medium (David & Durisen 1989) had taken into account the interaction with a relativistic particle component as a source of heating for the thermal plasma. However, we have finally chosen to neglect this specific contribution, although somehow appealing, since it is rather easy to show that, in the presence of a strong radiation field, such as the one we suppose emitted from a central source in the AGN and illuminating the wind, Compton interactions with radiation field photons would much more rapidly and substantially deplete the relativistic electron population of its energy, eventually going into the radiation field itself. Thus, on the one hand Compton losses would be the agent of a rapid evolution of the energy distribution function of a non-thermal relativistic component, and on the other hand they would render the contribution to the heating of thermal wind plasma due to collisional interaction with the injected relativistic electrons essentially negligible, even at the wind base. Comparing the energy loss rate for Compton interactions and that for collisional interactions, this is substantially true over the whole energy range (down to Lorentz factors $\gamma \sim 1$) of the non-thermal population energy distribution, for the conditions we would expect in a radio-quiet AGN. Therefore, contrary to the previously cited works, we have chosen to neglect this heating source for the wind plasma as both implausible, in the present context, and, especially, ineffective.

4.2. Radiative cooling rate

As for the radiative cooling rate $L_{\rm rad}(r,T) \equiv n^2\Lambda(T)$, we have started using a linear approximation of a numerically evaluated Cooling Function $\Lambda(T)$ (in erg cm^3 s^{-1}) for collisional ionization equilibrium, as described in Landini & Monsignori Fossi (1990); the cooling function can be represented linearly in a number of temperature ranges accurately chosen so as to obtain a good approximation of the numerically obtained functional behaviour.

Indeed, for the high temperature range, bremsstrahlung emission dominates the radiative cooling processes, and it turns out that for our high temperature wind plasma no significant difference in the solution is obtained if we just represent the cooling function with a much simpler approximation, only accounting for bremsstrahlung losses and neglecting line cooling contributions. The approximated expression we have used for the radiative cooling function is the following:

$$\Lambda(T)\ ({\rm erg\ cm^3/s}) = 2.1727 \times 10^{-27} T^{0.5}.$$

Moreover, although this is clearly a much more schematic representation of the cooling function, it actually seems even more appropriate, with respect to the one accounting for line cooling derived from purely collisional ionization equilibrium, for the present AGN context.

4.3. Compton interaction with the central radiation field

Since the thermal medium of the wind is illuminated by the centrally originated ionizing radiation field, we have to take into account the energy interactions between the electrons of the thermal plasma and the radiation field itself. Since our wind is endowed with sub-relativistic velocity, and we require for our solution to be of physical interest that the thermal wind is substantially optically thin to scattering processes, we can consistently use the well known relations giving energy gain and losses for the plasma due to Compton processes (Levich & Syunyaev 1971, Krolik et al. 1981; Begelman et al. 1983). For

a central isotropic source of luminosity L_0, we can write the energy loss rate per unit volume as

$$L_{\rm Comp} = \frac{n_{\rm e} k \sigma_{\rm T} L_0}{m_{\rm e} c^2 \pi r^2} T,$$

where n_e is the electron number density of the thermal wind plasma, *i.e.* the number density of the wind, since our wind is completely ionized, and the energy deposition rate per unit volume as

$$H_{\rm Comp} = \frac{n_{\rm e} k \sigma_{\rm T} L_0}{m_{\rm e} c^2 \pi r^2} T_{\rm Comp},$$

where $T_{\rm Comp}$ is the Compton temperature, defined as $T_{\rm Comp} \equiv < h\nu > /(4k)$, with $< h\nu > \equiv L_0^{-1} \int_0^\infty h\nu L_\nu d\nu$, and L_ν spectral luminosity of the central source (see Krolik et al. 1981, Begelman et al. 1983).

4.4. Parameterized heating rate contribution

A first analysis of possible complete solutions of our problem has shown that maintaining the wind "alive" on a large range of distances, that is obtaining a physical solution of the wind equations, is not at all easy (actually, it is not feasible), unless some other source of heating, possibly distributed all along the wind way, is taken into account. Also, we recall that in the case for an expanding spherical wind, expansion cooling turns out to be significant as to the temperature evolution, and its role can be important especially in the external region of the wind, where the flow velocity tends to be substantially constant. In spherical symmetry, rewriting the left hand side of Eq. (3) so as to make the temperature T of the plasma appear explicitly, the expansion cooling term in the energy balance equation is essentially expressed as $-2\rho v b T/r$, where $b \equiv 2k/m_{\rm H}$, and it is of course characteristic of an expanding flow. For a wind it is therefore impossible to maintain a gas temperature determined by the radiation field Compton temperature, $T_{\rm Comp}$, on a large distance range, since in any case the expansion cooling will act so as to decrease the temperature (Krolik & Begelman 1986). In particular, for the external region this implies that an extra heating term should be considered in order to keep a more or less constant value of the temperature itself.

We have therefore verified the necessity of accounting for some heating source for the wind plasma. One possibility is to try to include one or a combination of other possible heating mechanisms in the problem, implying the definition of the corresponding various physical scenarios. Another way around the problem is to try to define a parameterization, as simple as possible, for an additional contribution to the total heating rate, coming from an unspecified physical mechanism, so as to render the complete integration of the wind problem feasible (*i.e.*, obtaining non-diverging physical quantities), with a final result solution that effectively meets the physical basic requirements for an AGN wind. We have chosen this second method (see also Sect. 8.1), defining $H_* = H_*(r, T)$. This type of treatment of the problem, introducing an otherwise non-specified heating rate, is actually quite similar to the one adopted by other authors both in the AGN context (see Raine & O'Reilly 1993) and for the study of solar wind models (see Esser et al. 1997). The functional form of this additional heating rate is essentially the sum of a couple of different (*i.e.*, different spectral index and coefficient) power-laws (with respect to the radial distance r from the central black hole), one of which includes the possibility of a power-law dependence on the temperature as well and it reads:

$$H_*(r,T) = \left[C_1 \left(\frac{r}{r_{\rm g}} \right)^{\sigma_1} T^{k_{\rm T}} + C_2 \left(\frac{r}{r_{\rm g}} \right)^{\sigma_2} \right] \frac{\rho(r)}{r^2} \qquad (8)$$

where we need to specify the values of the various parameters, and $r_{\rm g} \equiv 2\frac{GM_{\rm BH}}{c^2}$ is the gravitational radius. Unless otherwise specified, the "physically sensible" solutions we have obtained correspond to an exponent $k_{\rm T} = 1$ for the temperature power-law.

5. Qualitative behaviour of winds

In this section, we want to mention a few general considerations relative to the temperature behaviour we can expect for a thermal AGN wind such as the one we are trying to model, accounting for the energetics we have described above.

If we are supposing a wind originating from a central region in which heating is released to the gas and a kind of corona is generated, of course we have to deal with the specific physical processes that come into play, but there are some very general qualitative lines of reasoning that should apply anyway. Close to a massive object, the physical conditions of the gas must compare with the escape velocity in the gravitational field of the object itself (see Begelman et al. 1983); in fact, a hot, nearly hydrostatic, non-magnetized corona can exist at a certain radius r_0, only if its temperature $T_{\rm cor}$ is such that the following condition is fulfilled

$$\frac{T_{\rm cor}}{T_{\rm g}} < 1,$$

where $T_{\rm g}$ is a gravitational "escape" temperature and it is defined (dimensionally equating thermal energy density to gravitational binding energy density) as

$$T_{\rm g} \equiv \frac{GM_{\rm BH}}{r_0} \frac{\mu m_{\rm H}}{k}.$$

Therefore, if the gas temperature is higher than the gravitational value defined above, the coronal gas sets up an expansion flow, because its pressure is larger than the gravitational energy density at that radius (r_0). In terms of velocity, this same condition can be expressed as

$$c_{\rm s}^2(r_0) > v_{\rm esc}^2(r_0),$$

where $c_{\rm s}(r_0)$ is the local sound speed at $r = r_0$, defined by $c_{\rm s}^2(r_0) = \gamma k T_{\rm cor}/(\mu m_{\rm H})$, and $v_{\rm esc}(r_0) \equiv (2GM_{\rm BH}/r_0)^{1/2}$, is the escape velocity at the same radius r_0; thus, for an expanding coronal flow to exist, it must be

$$T_{\rm cor} > \frac{3}{5} \frac{2GM_{\rm BH}}{r_0} \frac{\mu m_{\rm H}}{k} \equiv T_{\rm lim}.$$

If we suppose $r_0 = x_0 r_{\rm g}$, where $r_{\rm g} \equiv \left(2GM_{\rm BH}/c^2\right)$, and $x_0 = 30$ for example, we obtain

$$T_{\rm lim} = \frac{3}{5}\frac{c^2}{x_0}\frac{\mu m_{\rm H}}{k}, \tag{9}$$

that is $T_{\rm lim} = T_{\rm lim}(x_0) \simeq 10^{11}$ K. As a consequence, for a wind to emerge from the very central region of an AGN, its temperature at the base *must* be pretty high. The only way to circumvent this problem (that is to lower the base temperature of the wind) could be to accelerate the plasma, so that the wind does not set up due to thermal expansion only. To this purpose, momentum deposition at the base of the wind is required: the stronger this deposition is, the lower the temperature value that can be attained at the base of the wind.

A dimensional inspection of momentum and energy equations [Eqs. (2) ad (3)] allows an approximate discussion of the respective relevance of energy and momentum deposition. We shall restrict our attention to the case of constant mass flux, for simplicity.

The case for thermal expansion dominating the starting up of the wind has been discussed above, and corresponds to the situation in which the pressure gradient ($\sim \rho b T/r_0$, where we have set $b \equiv k/(\mu m_{\rm H})$) at the wind origin is stronger than the gravitational pull. In our momentum equation we have included radiation force momentum deposition as well as the possible contribution of momentum deposition due to those heating processes that imply the interaction with a relativistic and radially directed population of particles, namely H_*/c; this second contribution is not to be taken into account, at least in this simple form, when a different heating mechanism is supposed to be at work in the wind plasma (see Sect. 3).

Analyzing Eq. (2) one has to compare the gravitational term $-\rho_0 GM_{\rm BH}/r_0^2$ (where $\rho_0 \equiv \rho(r_0)$) with additional momentum deposition terms, $f_{\rm rad}(r_0)$ and $H_*(r_0)/c$), in case it is present.

Radiation force on the wind plasma of course helps lowering the temperature at the base of the wind, but its effects are not very conspicuous, since in any case the ratio between radiation force density and gravitational pull $f_{\rm rad}(r)/(\rho GM_{BH}/r^2)$ is in our case just $L_0/L_{\rm Edd}$, and this ratio, for the range of parameters here explored (which is typical of Seyfert 1s; see Table 1) is in the approximate interval $\sim 7\times10^{-2} \div 7\times10^{-3}$.

Therefore, a possibly relevant contribution to counteract gravitational attraction and lower the requirements on the inner temperature of the wind plasma for acceleration and expansion to take place can only be expected in the case in which the heating process is such to produce an associated momentum deposition (see Sect. 3), when this term, H_*/c, is sufficiently large. In this case, for a wind to be characterized by $T(r_0)$ significantly smaller than $T_{\rm lim}$, in principle it should be

$$H_*(r_0)/c \sim \rho_0 GM_{\rm BH}/r_0^2; \tag{10}$$

when this condition is fulfilled we would expect to have a wind set up without a huge value of the thermal pressure gradient, $\sim p/r_0$, required. Moreover, again in the case in which there is contribution to momentum deposition due to the heating process, an even more stringent limit condition that can be required to obtain lower values of the inner temperature of the wind is the following:

$$\left|\left(\frac{dp}{dr}\right)_{\rm r_0}\right| \sim \frac{p}{r_0} \ll \frac{H_*(r_0)}{c}. \tag{11}$$

Adding this condition to the previous one [relation (10)], a dimensional analysis of the energy equation can give more information. We refer to Appendix A for this analysis, and here we just summarize the indications we obtain. In the light of the considerations in Appendix A, when the two conditions (10) and (11) are simultaneously satisfied,we expect solutions that identify a class, or a "regime", characterized by temperatures in the inner region of the wind that are much lower than $T_{\rm lim}$, large density gradients with strong acceleration of the wind itself, and high inner region density. However, these properties suggest a closer and more attentive inspection of this class of solutions for what regards their "consistency" with respect to our basic requirements for the wind model (see Sect. 2), especially concerning the total optical depth expected for these solutions, that might well be larger than unity (see Sect. 8.1).

6. Wind equations and critical point definition

From the system of hydrodynamical equations written in Sect. 3, we can derive a system of two first order differential equations in two unknowns that we define as combinations of the original physical quantities, that is a) the sound speed $c_{\rm s}$, such that

$$c_{\rm s}^2 \equiv \gamma\left(\frac{p}{\rho}\right), \tag{12}$$

where $\gamma = 5/3$, and b) the Mach number M,

$$M \equiv \frac{v}{c_{\rm s}}. \tag{13}$$

The wind equations we obtain are the following:

$$\begin{aligned}
&\frac{M^2-1}{M^2}\frac{dM^2}{dr} = \\
&\frac{4}{r}\left(\frac{M^2}{3}+1\right) - \frac{8}{3}\frac{g}{c_{\rm s}^2} + \left(\frac{5}{3}M^2+1\right)\times \\
&\frac{2}{3}\frac{r^2}{Ac_{\rm s}^2}\left[\frac{\rho^2}{m_{\rm H}^2}\Lambda + L_{\rm Comp} - H_{\rm Comp} - H_*(1-v/c)\right] + \\
&\quad \frac{8}{3}M\frac{c_{\rm s}}{c}\frac{H_{\rm tot}r^2}{Ac_{\rm s}^2} - \frac{1}{f_{\rm m}}\frac{df_{\rm m}}{dr}\left[\frac{5}{3}M^2+1\right]\left[\frac{M^2}{3}+1\right],
\end{aligned} \tag{14}$$

$$\begin{aligned}
&\frac{M^2-1}{M^2}\frac{dc_{\rm s}^2}{dr} = \\
&-\frac{4c_{\rm s}^2}{3r} + \frac{2}{3}\frac{g}{M^2} - \frac{2}{3}\frac{c_{\rm s}}{Mc}\frac{H_{\rm tot}r^2}{A} - \left(\frac{5}{3}M^2-1\right)\times \\
&\frac{2}{3}\frac{r^2}{AM^2}\left[\frac{\rho^2}{m_{\rm H}^2}\Lambda + L_{\rm Comp} - H_{\rm Comp} - H_*(1-v/c)\right] +
\end{aligned}$$

$$\frac{c_{\rm s}^2}{M^2}\frac{1}{f_{\rm m}}\frac{df_{\rm m}}{dr}\left(\frac{5}{9}M^4-\frac{2}{3}M^2+1\right), \qquad (15)$$

where we have set $g \equiv M_{\rm BH}G/r^2$, and we remind that $A = A_0 f_{\rm m}(r)$, so that $(1/f_{\rm m})(df_{\rm m}/dr) = A'/A$. Similarly to what noticed at the end of Sect. 3 regarding the energy equation (3), the factor $(1 - v/c)$ multiplying H_* in both Eqs. (14) and (15) reduces to unity when the heating mechanism does not imply an associated momentum deposition H_*/c.

Since we are interested in wind-type flows, we are looking for transonic solutions, and specifically for those solutions starting from sub-sonic flow speed and getting to super-sonic; this of course means that the Mach number of the flow has to pass through the critical value $M = 1$, where the flow speed equals the local sound speed. To have a physically meaningful solution, we have to ask that, in the radial position at which it is $M = 1$, the radial derivatives of the physical unknowns $M(r)$ and $c_{\rm s}(r)$ maintain finite values; from the structure of the equations above, it is then clear that this condition is only attained if the right hand side of both the equations is set equal to zero at that same location; this in turn defines an implicit relation for the radial position at which the transonic transition takes place in the flow, that is the sonic (or critical) point, $r_{\rm c}$,

The sonic point position $r_{\rm c}$ is therefore obtained by the following implicit equation:

$$\frac{4}{r_{\rm c}}-\frac{8}{3}\frac{1}{f_{\rm c}}\left(\frac{df_{\rm m}}{dr}\right)_{\rm c}-\left(\frac{c}{c_{\rm sc}}\right)^2\frac{r_{\rm g}}{r_{\rm c}^2}+2\left(\frac{c_{\rm sc}}{c}\right)(H_{\rm rad})_{\rm c}\times$$
$$\frac{r_{\rm c}^2}{A(r_{\rm c})c_{\rm sc}^2}-\frac{4}{3}\frac{r_{\rm c}^2}{A(r_{\rm c})c_{\rm sc}^2}\Big[(H_*)_{\rm c}(1-5c_{\rm sc}/2c)+$$
$$(H_{\rm Comp}-L_{\rm Comp})_{\rm c}-\frac{\rho^2(r_{\rm c})}{m_{\rm H}^2}\Lambda_{\rm c}\Big]=0, \qquad (16)$$

where the subscript "c" indicates that the quantity is evaluated at the sonic point $r_{\rm c}$, $f_{\rm c} = f_{\rm m}(r_{\rm c})$, and $c_{\rm sc} = c_{\rm s}(r_{\rm c})$. From mass conservation equation (Eq. 1), one gets $A(r_{\rm c}) = A_0 f_{\rm m}(r_{\rm c}) = \rho(r_{\rm c})r_{\rm c}^2 c_{\rm sc}$; defining the dimensional constant as $A_0 \equiv \rho_{\rm c} r_{\rm c}^2 c_{\rm sc}$, we have $\rho_{\rm c} f_{\rm m}(r_{\rm c}) = \rho(r_{\rm c})$, and if there are no mass sources along the wind way, so that $A(r) = const. = A_0$, the constant $\rho_{\rm c}$ effectively represents the density of the wind at the sonic point. Again, in Eq. (16) the factor $[1 - 5c_{\rm sc}/(2c)]$ reduces to unity for the cases in which there is no momentum deposition contribution associated with the heating process represented by the parameterized heating rate H_*.

The critical point position is a function of general physical parameters of the problem (such as the mass of the central black hole $M_{\rm BH}$, the luminosity of the central source L_0 and the Compton temperature $T_{\rm Comp}$) of other parameters more specific to the chosen representation of the physical mechanisms determining heating and cooling rates, of the form of the non-dimensional mass deposition function $f_{\rm m}(r)$, and of the temperature at the sonic point itself, $T_{\rm c}$. The specification of these quantities defines the sonic point position. Notice that $r_{\rm c}$ does not depend on the value of $\rho_{\rm c}$, as it is clear from the non-dimensional version of the sonic point equation (Eq. (B.16)).

To build up the transonic solution we need then to integrate the wind equations starting from the sonic point, both inwards (towards the base of the wind at $r = r_0$) and outwards, up to the region where the wind has reached an asymptotic flow speed. This is actually possible by first expanding the equations around the sonic point to evaluate the derivatives of M and $c_{\rm s}$ at $r_{\rm c}$, as "initial" conditions for the integration. Appendix B shows the procedure and parameters for deriving non-dimensional equations to be numerically integrated.

To a first approximation, for the sub-relativistic wind solutions we are interested in and in the case in which the radiative cooling rate (in the region of the sonic point at least) is much smaller than the other energy exchange rates, *i.e.*, $\left((\rho^2/m_{\rm H}^2)\Lambda\right)_{\rm c} << (\rho(r_{\rm c})/r_{\rm c}^2)(\mathcal{F}_{\rm heat}-\mathcal{F}_{\rm cool})_{\rm c}$, where the subscript "c" implies the quantities are evaluated at the critical point $r_{\rm c}$ and we refer to Eq. (7) for the generic expression of energy exchange rates per unit volume, we obtain

$$r_{\rm c} \sim \frac{1}{4}\left(\frac{c}{c_{\rm sc}}\right)^2 r_{\rm g}+\frac{1}{3c_{\rm sc}^3}(\mathcal{F}_{\rm heat}-\mathcal{F}_{\rm cool})_{\rm c}. \qquad (17)$$

In order to obtain a wind solution, typically the dominant term is the first one, that is

$$\frac{1}{4}\left(\frac{c}{c_{\rm sc}}\right)^2 r_{\rm g}=\frac{1}{4}\frac{c^2}{\gamma b T_{\rm c}}r_{\rm g},$$

where again $b \equiv k/(\mu m_{\rm H})$, showing the dependence on the temperature value, while the energy rate balance term in Eq. (17) can be significant to move the sonic point farther away or closer to the central black hole, depending on whether, respectively, energy gain is larger than losses or viceversa.

7. Relativistic corrections

From the qualitative considerations on the temperature of the plasma of a nuclear AGN wind mentioned in Sect. 5, we do expect very high temperature values in the inner region of the wind. Indeed, the condition for the temperature T to reach values that are to be considered relativistic for the electron component of the plasma is that $kT/(m_{\rm e}c^2) > 1$, *i.e.* $T > 1.88 \times 10^9$ K; therefore, in the light of the discussion in Sect. 5, the electron component of the wind plasma can easily be characterized by relativistic temperatures, and such values are not much consistent with the use of totally non-relativistic equations, although the wind flow speeds are indeed sub-relativistic. As a consequence, we have appropriately modified the wind equations as it is described in the following of this section, and all the solutions that are explicitly described and shown in the present paper are those pertaining to the relativistically corrected problem.

In fact, although non-relativistic fluid motion is expected, relativistic temperatures require a relativistic treatment of energy density and energy exchanges, that is the use of a relativistically correct energy equation (see Landau & Lifshitz 1959).

In case of sub-relativistic fluid motion, the energy conservation equation can be formally written in the same way as for the non-relativistic case, as it is the case for the momentum equation (to $O(v/c)$ terms, which are of course negligible for our problem), that is

$$\frac{d\mathcal{E}}{dt}+(\mathcal{E}+p)(\nabla\cdot\mathbf{v})=\mathcal{G}-\mathcal{L}+\frac{v^2A'}{2r^2}, \qquad (18)$$

where $(d/dt \equiv \partial/\partial t + \mathbf{v}\cdot())$, $\mathcal{G}$ and $\mathcal{L}$ are, respectively, the total energy gain and total energy loss rates per unit volume, and where $\mathcal{E} = E_{\rm e} + E_{\rm p}$ is the total particle energy density; Eq. (18) is another form of the energy equation, and, in the totally sub-relativistic case, Eq. (3) in Sect. 3 can be easily derived from it. Here the difference with the non-relativistic case lies in the different expression for the relativistic electron energy density $E_{\rm e}$ and its relation to the thermal pressure p; also, it is important to stress that here $E_{\rm e}$ represents only the *kinetic* energy density of the relativistic electron component, due to thermal motions, that is it does not include the rest energy density.

Notice that here we only have to deal with relativistic electrons, since at the relevant temperature values the proton component of the plasma is still non-relativistic, and here we suppose that the electron and proton components have the same temperature. The total gas pressure expression for a completely ionized hydrogen gas is thus the same as in the non-relativistic case, namely, $p = p_{\rm tot} = 2n_{\rm th}kT = 2n_{\rm th}\Theta m_{\rm e}c^2$, that is the sum of the electron pressure and the proton pressure, where we have defined the non dimensional temperature parameter

$$\Theta \equiv \frac{kT}{m_e c^2}. \tag{19}$$

As for the energy density, we have the usual non relativistic expression for the proton component

$$E_{\rm p} = \frac{3}{2} n_{\rm th} kT = \frac{3}{2} n_{\rm th}\Theta m_{\rm e} c^2, \tag{20}$$

whereas the relativistic electron ("kinetic") energy density is

$$E_{\rm e} = n_{\rm th} K(\Theta)\Theta m_{\rm e} c^2 = K(\Theta) p_{\rm e}, \tag{21}$$

where $p_{\rm e}$ is the pressure of the electron component in the ionized gas, and $K(\Theta)$ is a function such that (see Björnsson & Svensson 1991, BS91 in the following)

$$K(\Theta)\Theta \equiv 3\Theta + \left[\frac{K_1\left(\frac{1}{\Theta}\right)}{K_2\left(\frac{1}{\Theta}\right)} - 1\right], \tag{22}$$

where K_1 and K_2 are modified Bessel functions of order 1 and 2 respectively and of argument $1/\Theta$, and the function $K(\Theta)$ has the following limit values

$$K(\Theta) \rightarrow \begin{cases} \frac{3}{2} & \text{for } \Theta << 1 \\ 3 & \text{for } \Theta >> 1 \end{cases}.$$

We can now express the relation between the total energy density $\mathcal{E}$ and the total gas pressure p as follows:

$$\mathcal{E} \equiv E_{\rm e} + E_{\rm p} = \left[\frac{K(\Theta) + 3/2}{2}\right] p = F(\Theta) p, \tag{23}$$

where we have defined

$$F(\Theta) \equiv (K(\Theta) + 3/2)/2. \tag{24}$$

With the definitions above, and using the continuity equation, which is still Eq. (1) since the fluid motion is sub-relativistic, one gets to a form of the energy equation perfectly analogous to Eq. (3), which is correct for the totally non-relativistic case:

$$\rho\left\{v\frac{d}{dr}\left[F(\Theta)\frac{p}{\rho}\right] + pv\frac{d}{dr}\left(\frac{1}{\rho}\right)\right\} = \mathcal{G} - \mathcal{L} + \frac{v^2 A'}{2r^2} - \frac{A'}{r^2}\left(\frac{\mathcal{E}}{\rho} + \frac{p}{\rho}\right); \tag{25}$$

this equation, together with Eqs. (1),(2) and (4), provides the system of hydrodynamic equations correct for relativistic electron temperature regime.

These equations can be combined to obtain a system of two equations in two unknowns, which are essentially the flow velocity and the temperature, representing a wind that is flowing at sub-relativistic speed, but whose plasma may be characterized by relativistic temperatures for the electronic component. Defining the following quantities

$$f_{\rm T}(T) \equiv \frac{dF}{d\Theta}\frac{d\Theta}{dT}T + F = \frac{dF}{dT}T + F \tag{26}$$

$$b \equiv \frac{2k_{\rm B}}{m_{\rm H}} \tag{27}$$

$$M_{\rm r}^2 \equiv \frac{v^2}{bT(1 + 1/f_{\rm T})} \tag{28}$$

$$K_{\rm M} \equiv \frac{M_{\rm r}^2 - 1}{M_{\rm r}^2} \tag{29}$$

$$\frac{A'}{A} = \frac{1}{f_{\rm m}}\frac{df_{\rm m}}{dr} \tag{30}$$

$$\mathcal{G} - \mathcal{L} \equiv H_*(1 - v/c) + H_{\rm Comp} - L_{\rm Comp} - \frac{\rho^2}{m_{\rm H}^2}\Lambda \tag{31}$$

$$P_{\rm M} \equiv K_{\rm M} + \frac{bT}{v^2 f_{\rm T}}, \tag{32}$$

we get the two equations for v and T

$$vK_{\rm M}\frac{dv}{dr} = \frac{2bT}{r}\left(1 + \frac{1}{f_{\rm T}}\right) - \frac{\mathcal{G} - \mathcal{L}}{\rho v f_{\rm T}} + \frac{H_{\rm tot}}{\rho c} - g - \frac{A'}{A}\left[v^2\left(1 + \frac{1}{2f_{\rm T}}\right) - bT\left(\frac{F}{f_{\rm T}} - 1\right)\right], \tag{33}$$

$$K_{\rm M}\frac{dT}{dr} = -\frac{2T}{r f_{\rm T}} + \frac{\mathcal{G} - \mathcal{L}}{\rho v f_{\rm T} b}P_{\rm M} - \frac{T H_{\rm tot}}{\rho v^2 f_{\rm T} c} + \frac{gT}{v^2 f_{\rm T}} + \frac{A'}{A}\left[\frac{v^2}{2bf_{\rm T}}\left(1 - \frac{2FbT}{v^2}\right)P_{\rm M} + \frac{T}{f_{\rm T}}\left(1 + \frac{bT}{v^2}\right)\right]. \tag{34}$$

We note again that, when the heating mechanism does not imply an associated momentum deposition, the factor $(1 - v/c)$, multiplying H_* in the definition of $\mathcal{G} - \mathcal{L}$ (Eq. (31)), reduces to unity.

The above representation of the problem is sufficient to our purposes. In fact, we are interested in wind solutions whose critical point temperatures, $T_{\rm c}$, are still in the non-relativistic range for the electrons and therefore we proceed by looking for the critical point of the wind in the non-relativistic regime, that is still using Eq. (16); then we obtain the wind solution,

first, that is close to the sonic point, by integrating equations (14) and (15), and then, going inwards to a region in which the temperature increases to finally reach the relativistic range for the electrons, by solving the system of relativistically corrected Eqs. (33) and (34), with the solution of the first step integration (non-relativistic equations) used as "initial" condition.

As a matter of fact, in writing down explicitly the expressions for energy gain $\mathcal{G}$ and losses $\mathcal{L}$ (energy density /time, dimensionally) we have to account for the fact that the electrons are in a relativistic regime; this turns out to change the rate at which energy is lost by the hot gas to the radiation field through Inverse Compton process, which is now $\propto T(1+4\Theta)$ (see Krolik et al. 1981), as well as the appropriate expression for the bremsstrahlung loss rate (see BS91), that turns out to be higher than what it would be if the non-relativistic, high temperature loss rate would be extrapolated up to relativistic temperatures. Thus, in the relativistic regime for electron temperatures, these rates turn out to have the following expressions:

$$L_{\rm Comp} \;=\; \frac{\rho(r)}{r^2}\left(\frac{k\sigma_{\rm T}L_0}{\pi m_{\rm p}m_{\rm e}c^2}\right)T(1+4\Theta), \tag{35}$$

$$\frac{\rho^2}{m_{\rm H}^2}\Lambda \;\equiv\; n^2\Lambda = \frac{3}{8\pi}(\alpha_{\rm f}\sigma_{\rm T}m_e c^3)n^2 f_\lambda(\Theta), \tag{36}$$

where for $(n^2\Lambda)$ we have taken into account the relativistic bremsstrahlung cooling rate for proton-electron interactions as given by BS91, $\alpha_{\rm f}$ is the fine-structure constant and the function $f_\lambda(\Theta)$ is given explicitly by BS91 as

$$f_\lambda(\Theta) = \begin{cases} (32/3)(2\Theta/\pi)^{1/2}(1+1.78\Theta^{1.34}) & \text{for } \Theta \le 1 \\ 12\Theta[\ln(1.12\Theta+0.42)+1.5] & \text{for } \Theta > 1. \end{cases} \tag{37}$$

We can now solve the wind problem consistently. However, to successfully integrate the relativistically correct system of equations and solve for the wind in its internal region, closer to its origin, we find that it is also necessary to modify the additional parameterized heating rate H_*, so that the portion of it which is dependent on T (see Eq. (8)) now is no longer simply linear with respect to T itself, but is instead $\propto T(1+\Theta)$ (similarly to the modification for "relativistically" correct Compton losses of the wind plasma). With this last change and choosing the values of the parameters appropriately, we can solve the equations in a consistent way and obtain physically sensible behaviour of the wind we are modeling.

We would like to stress at this point that all the considerations and dimensional analysis of Sect. 5 still apply for the relativistically correct case as well; in fact, in the energy equation (25), substituting non-relativistic Eq. (3), $F(\Theta)$ factors are of order unity or just a little larger than unity.

8. Wind solutions: a summary of results

8.1. General considerations on energetics and momentum deposition

We have already discussed the necessity of taking into account a parameterized heating rate to be able to obtain complete and sensible solutions for the stationary wind-type outflow problem analysed in the AGN context.

Inward resolution of wind equations, starting from the sonic point, is particularly critical from the energetics point of view, since we want to keep our model wind in the regime of well-behaved solutions, fulfilling the criteria we have identified in Sect. 2, that is that of tenuous, hot winds (see Sect. 5), representing a background connection for other denser and clumpy (line emitting or absorbing) AGN components. In fact, we expect temperatures in the inner region of the wind that can be easily much higher than the Compton temperature $T_{\rm C}$ for a typical AGN spectrum, that can be estimated around $10^7 \div 10^8$K (Krolik 1999). This leads to a very strong energy loss rate through Inverse Compton process for the wind plasma in favor of the radiation field photons. Thus, we have found that, to obtain a solution, a heating function (of unspecified origin at this level) is required essentially to avoid sort of an IC "catastrophe" that would stop a regular integration in the inner region. In the resolution of our problem, in particular, we have chosen a representative value $T_{\rm C} = 2\times 10^7$K for a broad-band spectrum, following Krolik 1988 (see also Mathews & Ferland 1987, Mathews & Doane 1990). We also tested different values of $T_{\rm C}$, to allow for possible different spectral distributions; however the wind models we present for the value mentioned above are quite representative of the typical results.

It seems here appropriate to stress the following issue. One of our wind requirements (Sect. 2) concerns the value of the total optical depth to scattering, that must be $\tau_{\rm T} \ll 1$, to be able to consistently neglect the consideration and the analysis of non-linear effects on the radiation field, that can be thus assumed to be substantially unaffected by the interaction with the nuclear wind through Compton processes. However, at the same time, from the point of view of the tenuous wind plasma, these same Compton interactions do have an absolutely significant role in the energetics of the plasma itself. This is not at all contradictory, and it is testified by the need for an heating source distributed along the wind way.

We have tried to compare the properties of our regular wind solutions with well known and simple wind models. An easy treatment is that of polytropic winds, in which case the energy equation is substituted by the assumption of a given simple relation between pressure and density of the wind gas, namely $p \propto \rho^\alpha$. In our energetic language, it can be shown that the conditions defined by such an assumption correspond to a situation in which the energy gain and loss mechanisms at work are such that the corresponding rates satisfy $\mathcal{G}-\mathcal{L} > 0$ (see Eq. (31) for the definition of $\mathcal{G}-\mathcal{L}$). In other words, this condition would be fulfilled for a model wind "mimicking" a simple polytropic wind, whose solution is guaranteed and behaviour well known. (Moreover, for a polytropic wind, it turns out that, whenever the wind is accelerating, $0 < \mathcal{G}-\mathcal{L} < 3c_{\rm s}^2\rho v/r$, which is of the order of the expansion cooling rate.) To our purposes this issue only represents an example, since our wind energetics is more complex, but also it again reinforces our choice of introducing an additional parameterized heating rate for the wind plasma with the aim of obtaining regular solutions.

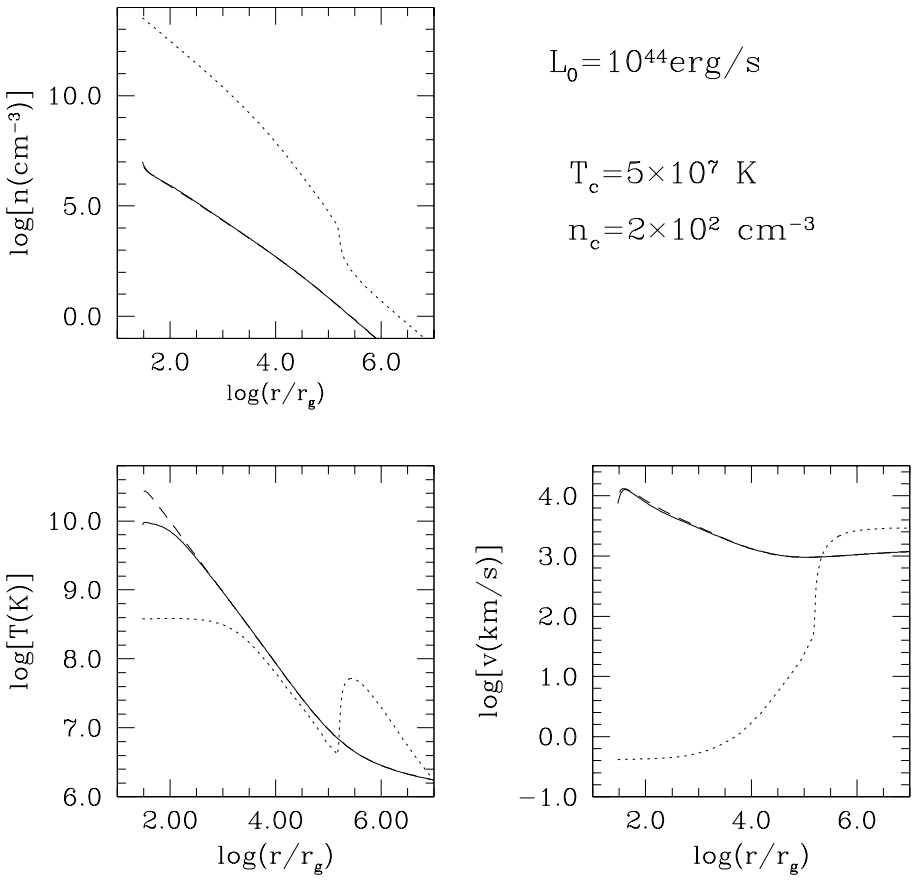

Fig. 1. Comparison between three different solutions, exemplifying three distinct classes of wind "models", as explained in detail in the text, and respectively represented by continuous, dotted, and dashed curves. Number density, temperature and outflow velocity behaviour are shown respectively in the three panels; parameters at the critical point are as specified in the figure; for all the three solutions $\sigma_1 = -0.03$ and $\sigma_2 = 1.0$. The only difference in parameters is in the respective values of C_1, that correspond to a ratio $C_1(\mathrm{dotted})/C_1(\mathrm{continuous}) \sim 200$, and $C_1(\mathrm{dashed})/C_1(\mathrm{continuous}) \simeq 1$.

For further qualitative discussion of wind energetics, we refer to Appendix A2, where more reasons supporting the necessity of an additional heating source distributed along the wind way for the construction of our AGN wind model are discussed. This heating source is represented by the parameterized heating rate described in Sect. 4.4 (with possible modifications as explained in Sect. 7). Our parameterization of this function could suggest a seemingly large freedom in the choice of the various parameters; this is however really only apparent, since, as a matter of fact, reasonable and complete solutions turn out to exist only when parameters are chosen within pretty narrow ranges of values. For the sake of completeness for the present considerations, we anticipate here part of the discussion of our choice of parameters, to which next section is devoted, namely that part regarding parameters that define $H_*(r,T)$. It turns out that the two parameters defining the spectral indices of the two power-laws (see Sect. 4.4) are restricted to the following values: $\sigma_1 \simeq -0.05 \div 0.$, and $\sigma_2 \simeq 0.7 \div 1.0$. As for the coefficients C_1 and C_2, they suffer strong limitations as well, C_1 especially, to perform inward integration of the equations; in fact, this last parameter must be appropriately chosen, since, once a solution is obtained for a certain value of C_1, variations of order $O(1)$ of this same value can prevent integration.

Fig. 1 shows three different examples of solutions of our problem, obtained for the case of constant mass flux, and identifying three distinct physical behaviours for the wind model; number density, temperature and velocity curves for the wind plasma are depicted in the three panels. The distinction among the three different classes of solutions that we exemplify in Fig. 1 is based essentially on the possible presence, value and relevance of a momentum deposition contribution H_*/c due to the heating mechanism. Indeed, the three solutions are obtained starting from the same set of parameters, except for the value of the heating rate coefficient C_1. Solid curves represent the physical quantities referring to a solution for which the energy deposition mechanism does require an associated momentum contribution to momentum deposition and the heating rate coefficient C_1 is within a rather narrow range, as mentioned in the previous paragraph. This type of solutions is characterized by rather low density and high temperature in the inner region of the wind (although significantly lower than $T_{\rm lim}$, as defined by Eq. (9) in Sect. 5, by at least one order of magnitude); the optical depth turns out to be $\tau_{\rm T} \ll 1$ and the total power exchanged in heating and cooling processes of the wind plasma is rather "low" (see below for a more quantitative characterization) with respect to the central radiation field luminosity L_0. These solutions, therefore, identify a regime of "consistency" with respect to the requirements of Sect. 2 for the AGN wind we intend to model, and in these cases the heating rate coefficient C_1 is such that the total "luminosity" $L_*(r_{\rm out})$ (where $r_{\rm out}$ is the outer integration radius) supplied to the wind by the heating source is

$$\int_{r_0}^{r_{\rm out}} H_*(r) 4\pi r^2 dr = L_*(r_{\rm out}) \lesssim L_0/10.$$

Still for energy deposition mechanisms implying an associated momentum deposition contribution, increasing C_1 by a minimum factor that can be as low as 5 (and increases with decreasing central source luminosity, to become as large as ~ 45 for $L_0 = 10^{43}\,\mathrm{erg\,s^{-1}}$) leads again to complete integration of the wind equations, but it produces the transition of the obtained solution to a markedly different regime for the model solutions; these are characterized by much lower inner temperatures and strong acceleration of the wind plasma, but strong density gradients and large inner region densities. This class of solutions is exemplified in Fig. 1 by the solution represented by the dotted curves and it corresponds to the regime we have qualitatively anticipated in Sect. 5. Once the solution is within this second regime, further increase of C_1 (*i.e.* of the heating rate and its associated momentum deposition rate), even by a very large factor, still produces a complete solution, with internal temperature that gets lower and lower; however, the resulting total optical depth values are very large, due to the large densities, and energy exchange rates for the energy deposition and loss processes turn out to be huge, confirming the qualitative considerations of Sect. 5. Our estimate of $L_*(r_{\rm out})$ for this example solution shown in Fig. 1 with the dotted curves gives, in fact, $L_*(r_{\rm out}) \sim 10^{50}\,\mathrm{erg\,s^{-1}}$, several orders of magnitude larger than the central source radiation field luminosity, which is a clearly unphysical value. Indeed, for these solutions, due to the correspondingly strong energy deposition rate in the wind plasma, especially close to its origin, momentum deposition from the H_*/c term is the dominant agent of the wind starting up and acceleration; since energy deposition is distributed in distance, acceleration of the wind goes on with r increasing, inducing a positive gradient of the flow velocity and a correspondingly strong negative gradient in the wind density, approaching the sonic point; in this first phase, the plasma temperature smoothly decreases, mostly due to expansion, and the additional heating tends to compensate radiative losses that (being $\propto \rho^2$) are the dominant energy loss mechanism. When the steep decrease in density brings radiative losses to be negligible with respect to heating, the wind temperature undergoes a rapid increase, just before the sonic point is reached. In the following supersonic region of the wind, because of the low density values reached, all the energy exchange processes are less relevant, and the physical quantities show a smooth behaviour.

On the contrary, the first solution discussed above, plotted with continuous curves, belongs to a regime in which thermal expansion still has a relevant role in starting up the wind, although momentum deposition helps to maintain the plasma temperature at the wind origin below the limiting value mentioned in Sect. 5, characteristic of pure "coronal expansion", and guarantees, at least close to the wind origin, an acceleration contribution for the wind plasma. In this case, the flow velocity profile is the result of a complex equilibrium between regions in which expansion slows down and others in which it accelerates, without anyway showing very large gradients.

The third solution shown in Fig. 1 and plotted with dashed curves is again obtained starting from the same set of physical parameters as the two previous ones, but refers to the the case in which there is no momentum deposition contribution due to the heating process. This is just the case in which, since the only momentum deposition is due to radiation force, the start up of the wind is dominated by thermal pressure driven expansion (see Sect. 5), and a temperature (much) closer to the limiting value $T_{\rm lim}$ discussed in Sect. 5 is expected; in fact, the value of the temperature at the base of the wind for the solution shown is $\sim 2.7 \times 10^{10}$ K. As a matter of fact, except for the behaviour of the temperature in the inner region (*i.e.* within $\sim 1000 r_{\rm g}$) of the wind, showing significantly larger values, this third model solution is quite similar to the one represented by continuous curves (and actually the density and velocity curves, as well as the temperature curve for $r \gtrsim 1000 r_{\rm g}$, are almost superimposed).

These two example solutions represent two opposite limit conditions as for the contribution to momentum deposition due to the heating process represented by H_* (see Sect. 3).

As already discussed, solutions in the "inconsistency" regime exemplified by the dotted curve solution are unacceptable following our criteria (see Sects. 2 and 5); on the other hand, the last type of solutions mentioned (exemplified by the dashed curve solution and characterized by no momentum deposition contribution due to the heating process) is also not very much promising, since the inner temperatures attained are really very high and imply very large energetic requirements.

Therefore, in the following sections we choose to examine in detail only the results pertaining to solutions in the regime exemplified by the solution represented with continuous curves in Fig. 1, in which a contribution to wind plasma acceleration is expected as a consequence of the heating process and for which the "consistency" and physical criteria of Sect. 2 are fulfilled.

Finally, we would like to just mention that in a first analysis we had taken thermal conduction as well into account; however, we have chosen to neglect it in our treatment, as it is apparent from the governing equations we have described in the previous sections, since thermal conduction turns out to be an efficient mechanism essentially when large gradients are present.

8.2. Physical parameters

We have analysed the physically interesting solutions for a sub-relativistic thermal wind-type flow originating in the very central regions of radio-quiet AGNs with a central luminosity source characterized by $L_0 = 10^{43} - 10^{44} - 10^{45}\,\mathrm{erg\,s^{-1}}$. We thus span the range of typical luminosities of Seyfert I galaxies. The present solutions are obtained by integrating the hydrodynamical equations as described in Sects. 3 to 7.

We have already mentioned the range of values explored as far as the luminosity of a central isotropic source is concerned. There are several other physical parameters that have to be set to solve for the wind-type outflow. As we have mentioned already, we have set the value of the radial distance from which the wind starts, i.e. the origin of the outflow as $r_0 = 30 r_{\rm g}$ (motivations of this choice are related to the limits for the central source dimensions derived from variability time-scales; see Koratkar & Blaes 1999).

Table 1. Gravitational parameters

$r_{\rm g}$ (cm)	$M_{\rm BH}$ ($M_\odot$)	$L_{\rm Edd}$ (erg s^{-1})	L_0 (erg s^{-1})	r_0 (cm)
3.333×10^{12}	1.12×10^{7}	1.46×10^{45}	10^{43}	10^{14}
1.667×10^{13}	5.62×10^{7}	7.31×10^{45}	10^{44}	5×10^{14}
3.333×10^{13}	1.12×10^{8}	1.46×10^{46}	10^{45}	10^{15}

We can actually divide model parameters into three groups. A first group refers to the AGN source parameters and it comprises the luminosity of the central source, L_0, whose values we have mentioned above and the gravitational parameters; as for these last, we have chosen different values of the central black hole mass ($M_{\rm BH}$) depending on the assumed value for the central source luminosity: increasing L_0 is associated with a larger value of $M_{\rm BH}$, as it is physically reasonable, and consequently with a larger value of $r_{\rm g}$ and of r_0 (since the ratio $x_0 \equiv r_0/r_{\rm g}$ is taken as constant). The values we have used for the solutions we present and discuss in the following are those appearing in Table 1. In this table we report the value of the Eddington luminosity, $L_{\rm Edd} = (4\pi G m_p c M_{\rm BH})/\sigma_{\rm T}$, corresponding to each adopted central mass: it is clear from the table that we did not assume a constant ratio $L_0/L_{\rm Edd}$. The present choice looks like reasonable, since central mass-luminosity relation in AGNs is still matter of debate, but at present it seems somewhat established that the ratio of luminosity to mass ($\propto L_0/L_{\rm Edd}$) is increasing with luminosity, and our values do follow this trend (see Wandel 1998).

A second group of parameters specifies the physical conditions at the sonic point, namely the values of $T_{\rm c}$, temperature of the wind plasma at $r_{\rm c}$, and $n_{\rm c}$, that is the number density of the wind at the critical point, $n(r_c)$, when no mass input along the wind is accounted for, whereas it gives $n(r_{\rm c})$ through the relation $n(r_{\rm c}) = n_{\rm c} f_{\rm m}(r_{\rm c})$ (see Sect. 6) when the wind is loaded by external mass along its way. The position of the sonic point is actually directly determined essentially by the chosen value of the temperature at the sonic point itself (see Eq. (17)): the higher is the temperature, the closer to the wind origin the outflow becomes supersonic.

Once defined these values, solutions depend on the choice of the parameters of a third group, those characterizing the additional parameterized heating rate function as defined in Sect. 4.4, and we have found that physically acceptable transonic solutions extending from the origin of the wind to the external asymptotic region of supersonic flow do exist only for a limited range of values of these last parameters, for a given choice of the ones previous described (see Sect. 8.1).

We have analysed different solutions, by changing the physical parameters, so as to meet the conditions imentioned in Sect. 2 as best as possible, and, consequently, to be able to identify the most favourable choices of the physical properties for the wind solutions themselves. The strongest restriction (as a matter of fact very significant for the effective existence of physically sensible solutions as well) turns out to be on the plasma density (characterized by the value of the parameter $n(r_{\rm c})$, the plasma number density at the sonic point); the wind density must be rather low, with typical values around a few 10^7 cm^{-3} at the wind base $r_0 = 30 r_g$. We have tried to analyze conditions under which the power input and/or exchange in the wind could be maintained much smaller than the total luminosity of the AGN, by varying the relevant parameters (especially those referring to the energetics of the problem), but it seems that to obtain a well behaved solution and meet the requirements above, we just need to keep the plasma density low.

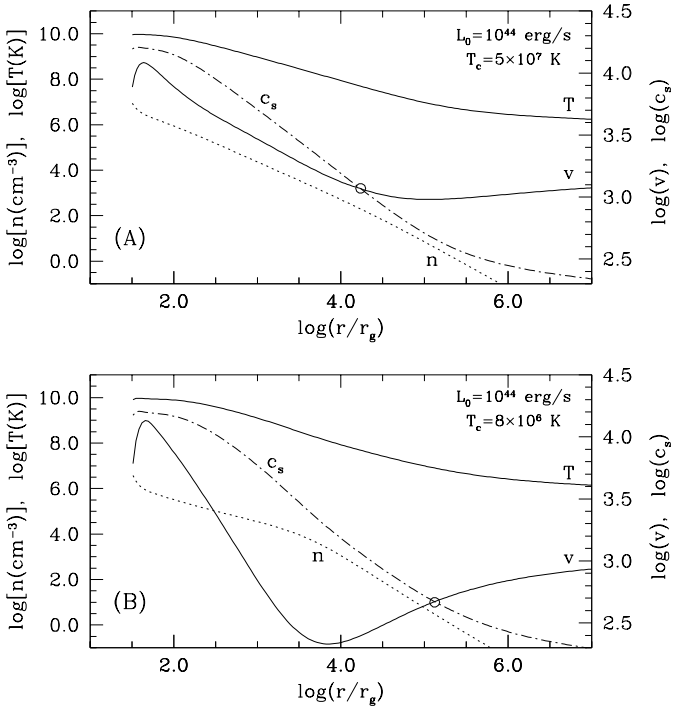

Fig. 2a and b. Panels **a** and **b** show the physical quantities for two wind models characterized by the same central luminosity and different values of the temperature at the critical point, as specified in plots; outflow velocity, v, and sound speed $c_{\rm s}$, are expressed in km s^{-1}; the circles drawn around the crossing point of outflow velocity and sound speed curves indicate the position of the sonic point. Solution in panel **a** is obtained with $n_{\rm c} = 2 \times 10^2$ cm^{-3} and $\sigma_1 = -0.03$, while for the solution in panel **a** it is $n_{\rm c} = 3$ cm^{-3} and $\sigma_1 = -0.04$; for both the solutions shown $\sigma_2 = 0.9$.

8.3. Solutions without mass input along the wind

We started looking for the existence of solutions in which the wind mass flux is constant along the wind itself, meaning that no external mass is entrained by the outflow. In our formalism (see Sect. 3), this implies we require that the mass flux per steradiant is $A(r) = A_0 = const.$ and the mass function $f_{\rm m}(r) = 1$.

Figs. 2 and 3 show four different solutions of this type, obtained starting from a different set of parameters and substantially representative of the behaviour of wind solutions of this type. In Fig. 2, we present two distinct solutions, shown in panels (A) and (B), referring to the same value of the central source luminosity, namely $L_0 = 10^{44}$ erg s^{-1}. In each of the two pan-

els, we plot the wind temperature and density, and the outflow radial velocity, as well as the sound speed as functions of the distance r from the central black hole, normalized to the gravitational radius $r_{\rm g}$; notice that this last quantity has the same value for the two solutions shown in Fig. 2, since they refer to the same central source luminosity and, thus, following our choice as shown in Table 1, to the same value of the central black hole mass, $M_{\rm BH}$. The small circle around the point in which the two curves for outflow velocity and sound speed cross each other indicates of course the critical point position for the outflow, becoming supersonic at larger distances. It is easily seen that for the wind solution (B), the one shown in the lower panel, the sonic point position is located much farther from the central black hole with respect to the sonic point characteristic of solution (A), in the upper panel. In fact, the main and more relevant difference between the parameters of the two solutions is the critical point temperature value, $T_{\rm c}$, which is chosen to be $T_{\rm c} = 5 \times 10^7$K for solution (A), whereas it is $T_{\rm c} = 8 \times 10^6$K for solution (B); as we have mentioned already in Sect. 6 and it can be directly seen from relation (17), sonic point temperature is the most significant parameter determining the sonic point of the wind, resulting in a position closer and closer to the wind origin for larger values of $T_{\rm c}$ itself.

Fig. 3 shows two more solutions, again identified as (A) and (B), respectively in the upper and lower panel, but this time the upper panel refers to a central luminosity $L_0 = 10^{45}\,{\rm erg\,s^{-1}}$, whereas the lower one shows a solution for a much smaller luminosity, $L_0 = 10^{43}\,{\rm erg\,s^{-1}}$, meaning that the central black hole mass is different as well (see Table 1). In this figure, we have chosen to plot solutions characterized by the same value of the critical point temperature, $T_{\rm c} = 5 \times 10^7$K, and the normalized values of the sonic point distance, $r_{\rm c}/r_{\rm g}$, are indeed not so different, although they do not coincide; this is, of course, due to the fact that "illumination" conditions for the wind plasma are very different, implying that heating and cooling conditions required to obtain the complete resolution of the wind problem can be different as well (see Eq. (17)), thus rendering somehow significant, to the sonic point determination, parameters that have in general only a secondary effect with respect to critical point temperature, $T_{\rm c}$.

All the solutions shown meet our selection criteria for consistency and physical significance. They are characterized by a small total optical depth to scattering, typically $\tau_{\rm T} \sim 0.002 \div 0.003$, except for the one wind solution for $L_0 = 10^{45}\,{\rm erg\,s^{-1}}$, for which we have a somewhat larger value $\tau_{\rm T} \simeq 0.015$, that is anyway still well within the "thin" regime. Power exchanges (gain or losses) for the wind plasma are also acceptable being at least one full order of magnitude (or even more) smaller than the luminosity of the central source.

A very general feature of the wind solution behaviour in the framework we have built up is the smoothness of the plasma temperature all along the explored extension of the outflow; wind temperatures are very high and, allowing for a very low and slowly decreasing heating rate component in the farthest, supersonic region (well beyond the BLR distance) of the wind, where its gas is very tenuous, the temperature can be easily

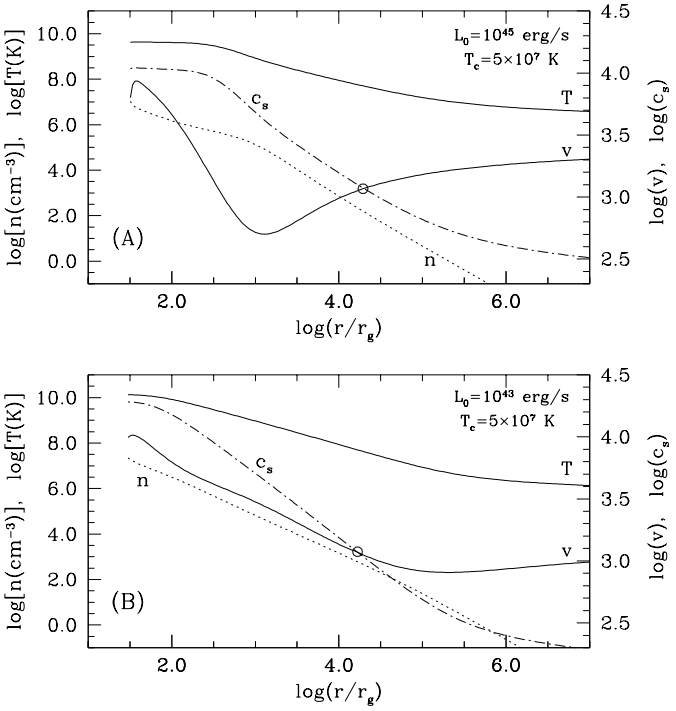

Fig. 3a and b. Panels **a** and **b** show the physical quantities for two wind models characterized by the same temperature at the critical point and different values of the central source luminosity, as specified in plots; outflow velocity, v, and sound speed $c_{\rm s}$, are expressed in ${\rm km\,s^{-1}}$; the circles drawn around the crossing point of outflow velocity and sound speed curves indicate the position of the sonic point. Solution in panel **a** is obtained with $n_{\rm c} = 1.5 \times 10^2\,{\rm cm^{-3}}$, $\sigma_1 = -0.015$ and $\sigma_2 = 1.0$, while while for the solution in panel **b** it is $n_{\rm c} = 6 \times 10^2\,{\rm cm^{-3}}$, $\sigma_1 = -0.03$ and $\sigma_2 = 0.9$.

kept around 10^6K or higher. This of course is consistent with our description of the wind gas as an essentially completely ionized plasma and with our rather schematic representation of radiation losses, since for such high temperatures radiation losses are substantially due to bremsstrahlung process.

Outflow velocity curves can be rather different depending on the solution, as can be seen comparing the solutions shown, although the outflow velocity values do not undergo strong variations. Decreasing critical temperature for given L_0, or increasing luminosity for a given critical temperature result in inducing the presence of a dip in the subsonic portion of the velocity curve, right before getting to the sonic point. This follows from the complex interplay of the various processes, mentioned in Sect. 8.1. Also, it influences directly the density behaviour, although this is not so immediate from the figures, due to the different scales chosen, since n and v are directly related by continuity equations (mass flux conservation equation) in the present case, in which no mass input along the wind is allowed for.

We have already discussed the necessity of maintaining the density parameters of the wind at low values; indeed, the wind density tends to decrease rather quickly, especially in the external regions, where the wind is accelerating again, or at best,

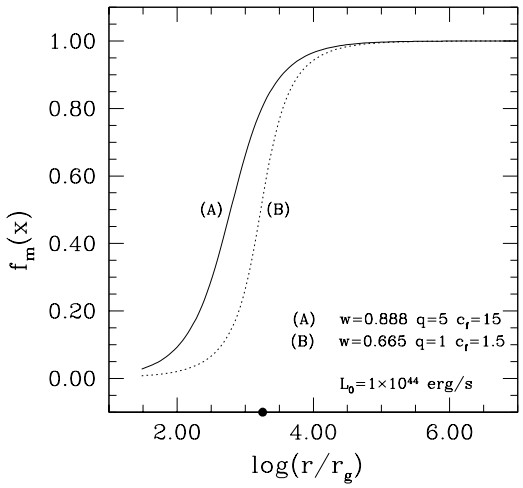

Fig. 4. Two examples of the mass input function $f_{\rm m}(x)$ as defined by Eq. (38) corresponding respectively to the two different choices of the set of parameters identified by the labels (A) and (B); notice that these two functions are respectively those chosen to build the wind models whose solutions are shown in the following Fig. 5 and labeled with the same (A) and (B) notation. The dot on the distance axis identifies the position of the reference BLR radius in units of $r_{\rm g}$, $x_{\rm BLR}$, as estimated in the text, for $L_0 = 10^{44}\,{\rm erg\,s^{-1}}$.

the outflow velocity is setting around its asymptotic value. The wind is therefore getting more and more tenuous with increasing distance from the inner region, so that it basically ends up to be almost physically "irrelevant"; unfortunately this may happen at distances that are comparable to those at which we deduce the presence of interesting phenomena, such as UV-X-ray absorption or even BLR. To circumvent this problem, we have examined wind models in which we allow for externally originated mass to be engulfed by the wind along the outflow, so as to try to maintain wind density around reasonable values even at large distances from the wind origin.

8.4. Solutions with mass input along the wind

Allowing for the mass flux per steradiant $A(r)$ to be effectively a function of distance and appropriately choosing the radial dependence of this function, we can build up wind models including a deposition of externally originated mass along the wind way. This has a twofold relevance. First, it allows to at least partially overcome the very low density problem we have just mentioned for constant mass flux solutions, when we consider the wind at large distances from the central source, since we allow for a mass input along the wind from a certain distance on, and this ends up in an increase of the wind density in the external regions of the outflow. Second, although we do not specify, here at least, the precise mechanism, it is pretty reasonable that a nuclear wind outflow, in which various other AGN components that are phenomenologically inferred to be at a certain distance from the central black hole are embedded, should have some sort of interaction with these components, and as a consequence, for example, entrain some mass to their expenses. This is in particular interesting with respect to the possible interaction/connection of this wind-type outflow with the physical component that gives origin to the well known broad emission lines, thus constituting the BLR. It is not the purpose of the present paper to model the relation between the nuclear wind we are studying and the BLR and to explore the details of their physical connection. This would, in particular, require also a specific model for the BLR itself, what is still matter of debate (see Korista 1999). We postpone this analysis to a subsequent paper (Torricelli-Ciamponi & Pietrini 2000), and in the present work we just start to study the characteristics of wind solutions with a mass deposition which is distributed along the wind essentially in a region more or less centered around the typical estimated distance for the BLR of an AGN of given luminosity L_0. The results we present all refer to the case with central source luminosity $L_0 = 10^{44}\,{\rm erg\,s^{-1}}$ and we estimate the BLR characteristic distance following the relation given by Netzer & Peterson (1997) and widely accepted, namely $r_{\rm BLR} \sim 0.01 L_{44}^{1/2}$ pc, where L_{44} is the central source luminosity in units of $10^{44}\,{\rm erg\,s^{-1}}$. We have built up a parameterized mass deposition function $f_{\rm m}(x)$, so as to mimic the desired behaviour of mass input along the wind. Its explicit form is the following:

$$f_{\rm m}(x) = 1 - w + \frac{2w}{\pi}{\rm arctg}\left[\left(\frac{x}{x_{\rm BLR}}c_{\rm f} - 1\right)\frac{1}{q}\right], \qquad (38)$$

where $x \equiv r/r_{\rm g}$, $x_{\rm BLR} \equiv r_{\rm BLR}/r_{\rm g}$ ($\simeq 1800$ for the presently chosen value for $L_0 = 10^{44}\,{\rm erg\,s^{-1}}$), and w,q, and $c_{\rm f}$ are three parameters whose adjustment allows us to obtain the required mass deposition. The mass flux difference between the wind origin and the asymptotic region in which mass deposition comes to be negligible is therefore

$$\Delta\dot{M}_{\rm w} = 4\pi A_0\,[f_{\rm m}(\infty) - f_{\rm m}(30)] = 4\pi A_0\,[1 - f_{\rm m}(30)]\,; \quad (39)$$

mass function parameters must therefore be chosen so as to both appropriately "center" the mass deposition and maximize the value of $\Delta\dot{M}_{\rm w}$, compatibly with other requirements for the AGN nuclear wind and with the supposed source of external mass, to obtain a non-negligible wind plasma density in the farthest wind regions. Fig. 4 shows the two different choices for $f_{\rm m}(x)$ that we have used to build the two exemplifying solutions with mass deposition that we present in Fig. 5; the labels (A) and (B) indicate that the corresponding mass function refers respectively to solution (A) or (B) in Fig. 5.

As for energy exchanges with entrained mass, since at this level we do not have any characterization of the thermal condition of this externally originated material, we have chosen not to model explicitly the energetics of the mass deposition in the wind; instead we simplify the problem by supposing that possible energy exchanges between the wind plasma and the deposed mass can be accounted for by our parameterized heating rate function $H_*(r)$.

A general consideration on this type of solutions is that increasing the wind plasma number density leads to an enhancement of the energetic requirements; in fact, ranges of parameters defining the energy deposition function that correspond to wind

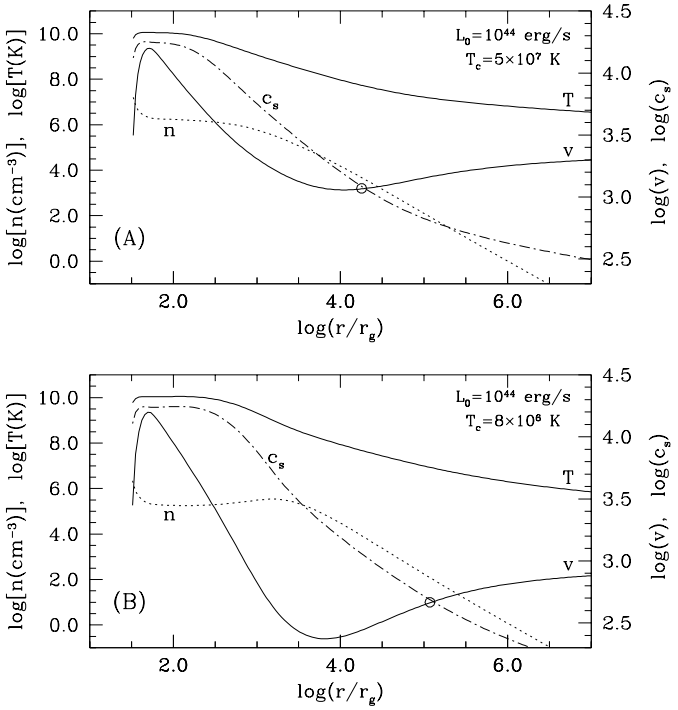

Fig. 5a and b. Two examples of mass-loaded wind models characterized by the same central luminosity and different values of the temperature at the critical point, as specified in the plots; outflow velocity, v, and sound speed $c_{\rm s}$, are expressed in km s^{-1}; the circles drawn around the crossing point of outflow velocity and sound speed curves indicate the position of the sonic point. Solution in panel **a** is obtained with $n_{\rm c} = 4 \times 10^3$ cm^{-3}, $\sigma_1 = -0.03$, and $\sigma_2 = 0.8$, while for the solution in panel **b** it is $n_{\rm c} = 10^2$ cm^{-3}, $\sigma_1 = -0.04$ and $\sigma_2 = 0.7$.

models whose properties are in the desired regime get even narrower than in the constant mass flux case.

Comparing the mass-loaded wind solutions in Fig. 5 with those for constant mass-flux in the analogous Fig. 2, the main difference lies of course in the number density curves (dotted lines); although starting substantially around the same values at the wind origin, for the solutions with mass-input we get rather flattened density curves in the regions of mass entrainment (whose extension can be identified by an inspection of Fig. 4). Indeed, for the solution in panel (B) there is actually a region around $(200 \div 1500) r_{\rm g}$ in which number density turns out to have a locally positive gradient as an effect of mass deposition. Beyond the distance at which the chosen mass deposition function $f_{\rm m}(x)$ reaches more or less its asymptotic value, i.e., the position from where on mass input is negligible, the density curves return to their steadily decreasing behaviour, but the global effect is that the density values in the external regions of the wind are significantly larger than those of the corresponding constant-mass-flux solutions (in Fig. 2), specifically by more than one order of magnitude in the examples shown. This is obtained still maintaining the solutions within the regime fulfilling our consistency criteria; in fact, for both the models shown, the resulting total optical depth to scattering is $\tau_{\rm T} \simeq 0.02$, and the total power exchanged by the wind plasma (for energy gains or losses) is still lower than L_0 by a good order of magnitude at least.

9. Conclusions or starting point? Our wind model and other components of a radio-quiet AGN

We have built a model AGN nuclear wind trying to account for the specific characteristics and physical processes relevant to the AGN phenomenon. Our model wind is of course quite schematic and in the present work we did not model explicitly its relation and interactions with other known AGN components. In Sect. 2, we discussed the basic hypotheses and requirements we have taken into account for the construction of this wind-type outflow in the AGN context; we refer to that section for details and here we just briefly recall them. Since we are interested in radio-quiet AGNs, we assume the flow must be sub-relativistic; also, the wind mass flux, $\dot{M}_{\rm w}$, is supposed to be much lower than the accretion mass flux, and, as a consequence, much lower than the critical accretion rate $\dot{M}_{\rm E}$. Moreover, we have required the wind to be optically thin to scattering, so that we can neglect the effects of Compton interactions between the wind plasma and the photons of the central source radiation field on the radiation field itself (although, as we have seen, the same Compton interactions are energetically very significant to the wind plasma); still with the aim of neglecting any possible variation of the central radiation field due to the existence of the wind, another request we have considered is that the wind's own emission (that is basically by bremsstrahlung, due to the high temperature of the plasma) is such to be negligible in luminosity with respect to that of the central source.

We found out that a stationary, non-magnetized wind-type outflow, satisfying the conditions above, can exist in an AGN under rather specific conditions, that is, although we have several parameters that come into play for the model definition, the range of parameters allowing for a complete and physically consistent solution of the wind problem is always quite narrow.

However, our results do seem to be encouraging, since there are several observational hints for the actual presence of material outflowing from the central regions of radio-quiet AGNs, and we have started to define more precisely under what physical conditions such outflows can be expected.

We have analyzed hydrodynamic and energetic conditions allowing for the resolution of the stationary wind problem.

Recalling briefly Sect. 8.1 results, one of these conditions is the necessity of a heating source for the wind plasma, distributed in radial distance and proportional to the plasma density; we have introduced it in terms of a parameterized heating rate $H_*(r)$, and we have shown its importance from the energetic balance point of view both for the transonic region of the wind, where the solution is the result of the complex balance of energy deposition/loss and momentum deposition as well, and for the outer supersonic region, where the wind behaviour is more similar to that of a polytropic-like wind, for which the energetic balance must be $\mathcal{G} - \mathcal{L} > 0$. We have modeled $H_*(r)$ in a parameterized form, but we have not yet identified its physical

origin, that is certainly an issue to be clarified in the context of radio-quiet AGN physics (see Sect. 4).

In the chosen descriptive framework, rather strict requirements turn out to be imposed on the parameters defining this heating function H_*.

We have found that we can build model winds that are characterized by very high temperatures (up to relativistic values for the wind plasma electrons close to the wind origin) in the inner regions, and external (supersonic) zone temperatures that can be easily maintained high enough to ensure complete ionization of the wind plasma ($T_{\rm out} \sim 10^6$K). Also, the wind turns out to be rather tenuous, with plasma number density at the wind origin that is typically around a few$\times 10^7$ cm^{-3} and then decreases so that, for a constant mass flux wind, the outer supersonic regions of the wind are extremely rarefied, what makes the wind almost unsubstantial.

To circumvent this problem so as to account for possible interactions of the wind with other physical components of the AGN central region, leading to external mass entrainment in the outflow, we have devised a simple treatment for the inclusion of a distributed mass source along the wind way. We have thus built up wind models with non-constant mass flux, increasing with radial distance in a given region, whose extension and location we can appropriately define. The resulting outer plasma density can be therefore maintained at larger values.

The consideration of mass-loaded wind models also allows us to attack the issue of the relationship between the nuclear hot wind, as a kind of background, and other interesting phenomenological components of the AGN central region. In fact, on one hand we can relate the origin of the external mass input for the wind to the presence of a clumpy line emitting component as the BLR, with which the wind interacts, somehow entraining part of its material; on the other hand, wind models with non-negligible density values at "large" distances, that is distances comparable with the inferred estimates of the position of outflowing UV absorbers, allow us to examine the possible relation of our wind with these UV(-X-ray) absorbers as well.

As for the relation with the BLR, we postpone this study to a forthcoming paper (Torricelli & Pietrini 2000); here we just mention that we are going to study this problem within the framework of those models that structure the BLR with a central compact star cluster, whose evolved stars (the so-called "bloated" stars) originate gas envelopes and stellar winds that can be both considered the site of the line emission and the source of mass for wind entrainment [see Korista (1999) for a general review, and Alexander & Netzer (1994), Alexander & Netzer (1997) and Alexander (1997) for a recent model of "bloated"-star BLR].

The relation with UV and X-ray absorbers, quite commonly present in Seyfert galaxies (Crenshaw et al. 1999) should be explored as well. We find encouraging the fact that the physical properties of our mass-loaded wind models at the estimated (model dependent) distances of these AGN components are such that, for example, the wind thermal pressure ($\propto nT$) is comparable or anyway within the range of estimated values of the thermal pressure of these absorbers. Moreover, at these same distances our wind-type outflow models can have a velocity quite similar to the values of outflow velocity of the UV-absorbers (at least for what regards Seyfert 1s) estimated from spectroscopic analysis of the blueshift of the observed absorption lines, i.e. $v_{\rm wind} \simeq v_{\rm UVabs}$.

These results would suggest a possible relation between a background nuclear wind as the one we have modeled and these phenomenological components of AGNs. The nature of this relation is at present not defined. However, in the framework of models in which UV absorbers are due to clumpy material embedded in a surrounding medium, a possible speculation, suggested by the order of magnitude pressure equilibrium between our wind-type outflow and the absorbing material, could be that the absorbing clumps are somehow dragged along by the wind itself, identified with the background medium, and they are essentially comoving with the wind, thus avoiding the disrupting effects of hydrodynamical instabilities. In this case, substantial thermal pressure equilibrium would be achieved thanks to the conspicuous local values of the wind temperature and to the fact that the input of external mass, that we suppose to take place at BLR distances, guarantees appropriate (sufficiently large) wind density at UV absorber distances. This would be obtained without requiring too large mass loss rate from the very central region (*i.e.*, close to the wind origin) (see de Kool 1997).

To be more specific, we have to recall, first of all, that, apart from this spectroscopic determination of the outflow velocity of the UV-absorbers, the estimates of the distance and of other physical properties of the absorbing material, such as density and temperature, that are found in literature do depend on the assumed photoionization model through which the authors analyse the observations. The estimated distances typically range from $\sim$ 50ld to $\lesssim 1$ pc, and the order of magnitude of the thermal pressure, given as nT, is around 5×10^8Kcm^{-3} and 2×10^{10}Kcm^{-3}, assuming temperatures in the range $10^4 \div 10^5$K; see, for example, the studies on NGC3516 by Mathur et al. (1997) and on NGC5548 by Mathur et al. (1995), and by Crenshaw & Kraemer (1999). From these same authors and references therein, an estimate of the outflow velocity of the UV absorbing material of Seyfert galaxies gives $v_{\rm UVabs} < 2000\,{\rm km\,s^{-1}}$, and, more specifically, for the two AGNs mentioned above, it is $v_{\rm UVabs} \sim 500\,{\rm km\,s^{-1}}$ (for NGC3516) and $v_{\rm UVabs} \lesssim 1000$–$1200\,{\rm km\,s^{-1}}$ (for NGC5548).

An inspection of the two example solutions for the case of mass-loaded wind models shown in Fig. 5, both corresponding to $L_0 = 10^{44}\,{\rm erg\,s^{-1}}$, allows us to verify that for both the solutions nT is in the range of estimated order of magnitude of the UV-absorber thermal pressure mentioned above between $4 \times 10^4 r_{\rm g}$ and $17 \times 10^4 r_{\rm g}$, corresponding to the interval between $\sim$ 260ld and $\sim$ 1100ld, which is right within the range of estimated distance of the UV-absorber component. Also, it is interesting to notice that, in this range of distances, the wind outflow velocity is between ~ 1200–$1500\,{\rm km\,s^{-1}}$ for the solution in panel (A) of Fig. 5, whereas for the one shown in panel (B) it is ~ 350–$500\,{\rm km\,s^{-1}}$; again these values seem to match rather well the observed values of $v_{\rm UVabs}$.

Of course, the considerations above are purely speculative at present, but they are stimulating to start the analysis of the possible role of a nuclear wind such as the one we have studied in the present paper in understanding the scenario of UV-X-ray absorbers in AGNs. This is postponed to future work.

Acknowledgements. This work was partly supported by the Italian Ministry for University and Research (MURST) under grant Cofin98-02-32

Appendix A: qualitative issues on wind energetics

A.1. Energetics and momentum deposition

The following analysis refers to the case in which the energy deposition process implies a corresponding momentum deposition contribution (see Sects. 3 and 5). Since we are interested in analyzing winds with internal temperatures much lower than the huge value of $T_{\rm lim}$ we have estimated above, we look for the consequences on the energy equation of the limit conditions (10) and (11) of Sect. 5. In the constant mass flux limit, and supposing that, given the first of the conditions above, we can approximate with H_* the whole of the energy balance (gain minus loss rates) appearing on the right hand side of the energy equation (Eq. (3)), this same equation, divided by c, can be rewritten, close to the wind origin, as

$$\frac{v}{c}\frac{1}{\gamma-1}\frac{dp}{dr}-\frac{\gamma}{\gamma-1}\frac{p}{\rho}\frac{1}{c}\frac{d\rho}{dr}\sim\frac{H_*}{c}.$$

Since the second of conditions (10) must apply (and the more so $(v/c)(dp/dr)\ll H_*/c$, because the flow is sub-relativistic), this equation leads to the condition

$$-\frac{\gamma}{\gamma-1}\frac{p}{\rho}\frac{1}{c}\frac{d\rho}{dr}\sim\frac{H_*}{c},$$

or, neglecting the factor of order unity $\gamma/(\gamma-1)$,

$$-\frac{p}{r}\frac{d\ln\rho}{d\ln r}\sim-\left|\frac{dp}{dr}\right|\frac{d\ln\rho}{d\ln r}\sim\frac{c}{v}\frac{H_*}{c}.$$

From this relation we can conclude that, allowing for small dp/dr and large momentum deposition H_*/c, we can expect very large gradients in density in the inner wind region, that, no matter what is the value of the density itself at the distance at which the wind becomes supersonic, lead to a very large density in the internal region. This in turn can easily imply a total optical depth to scattering that is by far exceeding unity (by orders of magnitude) and resulting total power exchanges in the energy deposition and loss processes that are very large with respect to the central source luminosity; as a consequence, in this case the corresponding solution would turn out to be unacceptable with respect to our criteria, and inconsistent as for our treatment.

A.2. Energy balance

In Sect. 8.1 we have discussed the importance of an additional heating source distributed in distance along the wind way for a wind model, mentioning the well known case of simple polytropic models, corresponding to a situation in which the energetic balance ($\mathcal{G}-\mathcal{L}$) is in favour of energy gain. Nevertheless, we do expect our wind model energetics to be more complex than that of a wind resembling a simple polytropic model. In fact, exploring the parameter space to understand and identify the conditions to effectively get well-behaved solutions, we have found that the parameters chosen to define $H_*(r,T)$ are pretty critical and determine a rather narrow range, if we want to keep our solution in the physically reasonable regime (see Sect. 5). Moreover, an inspection of the energetics shows that for our model the balance $\mathcal{G}-\mathcal{L}$ can locally be <0, although, in general, when this is verified, the relative value of the difference is quite small, *i.e.* $|\mathcal{G}-\mathcal{L}|/\mathcal{L}\ll 1$.

Our model is closer to a polytropic-mimicking wind in its supersonic, external region, where $dv/dr\gtrsim 0$ and, in the asymptotic limit, $dv/dr\simeq 0$; in this case, in fact, it is always $\mathcal{G}-\mathcal{L}>0$, and also, due to the very small densities reached in this region, it can be $|\mathcal{G}-\mathcal{L}|/\mathcal{G}\sim O(1)$. Indeed, for a model with constant mass flux, combining Eqs. (2) and (3) (non-relativistic energy equation is of course appropriate for the description of this supersonic region) in the asymptotic limit, in which $dv/dr\simeq 0$ and for $r\gg r_{\rm c}$, we get

$$(\mathcal{G}-\mathcal{L})>\frac{1}{\gamma-1}v\frac{(H_*+H_{\rm rad})}{c}>0.$$

In this region, even for negligible H_*, it is $\mathcal{G}-\mathcal{L}>0$, since at these distances, being $T<T_{\rm Comp}$ and the density of the wind very low, $H_{\rm Comp}>(n^2\Lambda+L_{\rm Comp})$; however, in this case, the wind temperature tends to decrease, since the expansion cooling term ($\propto T/r$) is decreasing more slowly than $H_{\rm Comp}/\rho\propto T_{\rm Comp}/r^2$. Thus, to avoid a too strong decrease of the temperature in this external region or to maintain a sort of asymptotic, more or less constant (or slowly decreasing) temperature, the contribution of H_* is again necessary, and it must be $H_*/\rho\propto 1/r$ or a close power of r.

Appendix B: non-dimensional parameters and equations

In this Appendix, we explicitly describe our choice for normalization of the physical quantities appearing in the wind equations derived in Sect. 3.

Apart from the Mach number $M\equiv v/c_{\rm s}$, which is non-dimensional due to its own definition, all the physical quantities appearing in the wind equations are dimensional, and we have to reduce them to the corresponding non-dimensional ones with a normalization appropriate for our problem. A natural choice for a wind problem, in which the sonic point is a critical starting point for the resolution of the problem itself, is to build up the normalization of the problem making use of the chosen physical parameters at the sonic point itself, namely $T_{\rm c}=T(r_{\rm c})$, and $\rho_{\rm c}=\rho(r_{\rm c})/f_{\rm m}(r_{\rm c})$, which is directly the value of the density at the critical point only if $f_{\rm m}(r_{\rm c})=1$, what is for sure verified when no mass sources along the wind are taken into account.

From the temperature at the critical point, $T_{\rm c}$, we obtain the sound speed at the critical point itself, since

$$c_{\rm sc}^2 \equiv c_{\rm s}^2(r_{\rm c}) = \gamma \left(\frac{2k}{m_{\rm H}}\right) T_{\rm c}, \tag{B.1}$$

where $\gamma = 5/3$. We choose however to normalize distances with the gravitational radius $r_{\rm g} \equiv 2GM_{\rm BH}/c^2$, to account for a basic ingredient in the problem such as the central black hole gravitational pull. We thus define the following non-dimensional quantities:

$$x \equiv \frac{r}{r_{\rm g}}, \qquad \overline{T}(x) = \frac{T}{T_{\rm c}} \tag{B.2}$$

$$s(x) \equiv \frac{c_{\rm s}}{c_{\rm sc}} = \sqrt{\overline{T}} \tag{B.3}$$

$$\overline{\rho}(x) = \frac{\rho}{\rho_{\rm c}}; \tag{B.4}$$

from the definitions given in Sect. 3, the non-dimensional mass flux per steradiant can be written as

$$\overline{A}(x) \equiv \frac{f_{\rm m}(x)}{A_0} = \frac{f_{\rm m}(x)}{\rho_{\rm c} r_{\rm c}^2 c_{\rm sc}}, \tag{B.5}$$

so that the non-dimensional wind density can be recovered from the results of integration for $M = M(x)$ and $s = s(x)$ as

$$\overline{\rho}(x) = \frac{x_{\rm c}^2 f_{\rm m}(x)}{x^2 M s}, \tag{B.6}$$

where, of course, $x_{\rm c} \equiv r_{\rm c}/r_{\rm g}$.

As for the energy exchange rates per unit volume, for those that can be written in the form defined by Eq. 7 in the paper ($H_\star(x)$, $H_{\rm Comp}(x)$, $L_{\rm Comp}(x)$, and the quantity $H_{\rm rad}(x)$, defined by Eq. 5 and related to radiation pressure momentum deposition in the wind), we can isolate a dimensional factor $\left(\rho_{\rm c} c_{\rm sc}^3/r_{\rm g}\right)$, so that the non-dimensional corresponding quantity can be expressed as

$$\overline{\mathcal{H}}(x) = \left(\frac{\rho_{\rm c} c_{\rm sc}^3}{r_{\rm g}}\right)^{-1} \mathcal{H}(x), \tag{B.7}$$

that is

$$\overline{\mathcal{H}}(x) = \frac{\overline{\rho}(x)}{x^2}\overline{\mathcal{F}}(x) = \left[\frac{x_{\rm c}^2 f_{\rm m}(x)}{x^4 s M}\right]\overline{\mathcal{F}}(x), \tag{B.8}$$

where $\overline{\mathcal{F}}(x) \equiv \mathcal{F}(x)/(r_{\rm g} c_{\rm sc}^3)$ is the non-dimensional version of the characteristic rate function $\mathcal{F}(x)$. To be more specific, we have

$$\overline{H}_\star(x) = \frac{\overline{\rho}(x)}{x^2} h_\star(x) = \frac{\overline{\rho}(x)}{x^2}\left(\overline{C}_1 \frac{s^{2k_{\rm T}}}{x^{-\sigma_1}} + \overline{C}_2 x^{\sigma_2}\right), \tag{B.9}$$

$$\overline{H}_{\rm Comp}(x) = \frac{\overline{\rho}(x)}{x^2} h_{\rm Comp} = \frac{\overline{\rho}(x)}{x^2}\left(D_0 \frac{T_{\rm Comp}}{T_{\rm c}}\right), \tag{B.10}$$

$$\overline{L}_{\rm Comp}(x) = \frac{\overline{\rho}(x)}{x^2} l_{\rm Comp} = \frac{\overline{\rho}(x)}{x^2}\left(D_0 s^2\right), \tag{B.11}$$

$$\overline{H}_{\rm rad}(x) = \frac{\overline{\rho}(x)}{x^2} h_{\rm rad} = \frac{\overline{\rho}(x)}{x^2}\left(\frac{\sigma_{\rm T} L_0}{4\pi m_{\rm p} c_{\rm sc}^3 r_{\rm g}}\right), \tag{B.12}$$

where $\overline{C}_1$ and $\overline{C}_2$ are two non-dimensional parameters,

$$D_0 \equiv \left(\frac{\sigma_{\rm T} L_0}{2\pi m_{\rm e} c^2 \gamma c_{\rm sc} r_{\rm g}}\right),$$

and other quantities appearing in the definitions above have been introduced in the sections referring to the heating and cooling rates in the text.

The same dimensional factor can be of course used to obtain the non-dimensional radiative cooling rate per unit volume from $(\rho^2/m_{\rm H}^2)\Lambda$, for which we have in fact

$$\frac{\rho^2}{m_{\rm H}^2}\Lambda \equiv n^2\Lambda = \left(\frac{\rho_{\rm c} c_{\rm sc}^3}{r_{\rm g}}\right)\left[\overline{\rho}^2(x)\lambda(s^2)\right], \tag{B.13}$$

where the quantity in square parentheses is the non-dimensional rate per unit volume.

B.1. Normalized form of non-relativistic wind equations

Making use of the definitions above, we obtain the non-dimensional form of Eqs. (13) and (14):

$$\frac{M^2-1}{M}\frac{dM}{dx} = \frac{2}{x}\left(\frac{M^2}{3}+1\right) - \frac{2}{3}\frac{1}{s^2x^2}\left(\frac{c}{c_{\rm sc}}\right)^2 + \left(\frac{5}{3}M^2+1\right)\times \frac{1}{3Ms^3x^2}\left[\frac{x_{\rm c}^2 f_{\rm m}}{Ms}\lambda + l_{\rm Comp} - h_{\rm Comp} - h_*(1 - Msc_{\rm sc}/c)\right] + \frac{4}{3}\frac{c_{\rm sc}}{c}\frac{h_{\rm tot}}{s^2x^2} - \frac{1}{2}\frac{1}{f_{\rm m}}\frac{df_{\rm m}}{dx}\left[\frac{5M^2}{3}+1\right]\left[\frac{M^2}{3}+1\right], \tag{B.14}$$

$$\frac{M^2-1}{s}\frac{ds}{dx} = -\frac{2M^2}{3x} + \frac{1}{6s^2x^2}\left(\frac{c}{c_{\rm sc}}\right)^2 - \left(\frac{5}{3}M^2-1\right)\times \frac{1}{3Ms^3x^2}\left[\frac{x_{\rm c}^2 f_{\rm m}}{Ms}\lambda + l_{\rm Comp} - h_{\rm Comp} - h_*(1 - Msc_{\rm sc}/c)\right] - \frac{1}{3}\frac{c_{\rm sc}}{c}\frac{h_{\rm tot}}{s^2x^2} + \frac{1}{2}\frac{1}{f_{\rm m}}\frac{df_{\rm m}}{dx}\left(\frac{5M^4}{9} - \frac{2M^2}{3} + 1\right), \tag{B.15}$$

where the non-dimensional functions $h_\star(x)$, $h_{\rm tot}(x) = h_*(x) + h_{\rm rad}$, $h_{\rm comp} \propto T_{\rm Comp}/T_{\rm c}$, and $l_{\rm Comp} \propto s^2$ represent the various rate functions $\overline{\mathcal{F}}$ defined generically by Eq. (B8), corresponding to the energy exchange rates per unit volume labeled with the same subscript; $\lambda = \lambda(s^2)$ is the normalized cooling function as defined by Eq. (B.13)

Also, the normalized sonic point ($x_{\rm c} \equiv r_{\rm c}/r_{\rm g}$) implicit equation is corresponding to Eq. (15)

$$\frac{4}{x_{\rm c}} - \frac{8}{3}\frac{1}{f_{\rm c}}\left(\frac{df_{\rm m}}{dx}\right)_{\rm c} - \left(\frac{c}{c_{\rm sc}}\right)^2\frac{1}{x_{\rm c}^2} + 2\left(\frac{c_{\rm sc}}{c}\right)\frac{(h_{\rm rad})_{\rm c}}{x_{\rm c}^2} - \frac{4}{3x_{\rm c}^2}\left[(h_*)_{\rm c}\left(1 - \frac{5c_{\rm sc}}{2c}\right) + (h_{\rm Comp} - l_{\rm Comp})_{\rm c} - x_{\rm c}^2 f_{\rm c}\lambda_{\rm c}\right] = 0. \tag{B.16}$$

B.2. Normalized form of relativistically correct wind equations

Relativistically corrected equations of Sect. 7 have to be reduced to their non-dimensional form. Our choices for normalization of the various dimensional quantities are the same defined at the beginning of the present Appendix B, except for velocity normalization; here we define a non-dimensional velocity by making use of the sound speed at the critical point, $c_{\rm sc}$, which is still given by Eq. (B.1), so that

$$u \equiv \frac{v}{c_{\rm sc}}; \tag{B.17}$$

notice that, since,as we have mentioned in Sect. 7, the temperature value at the critical point for the solutions we are interested in is always chosen in the non-relativistic range, the definition of the sound speed at the critical point is always the one given in Eq. (B.1) and it keeps it physical meaning in any case. With this notation, the expression for the normalized gas density now turns out to be

$$\overline{\rho}(x) = \frac{x_{\rm c}^2 f_{\rm m}(x)}{x^2 u}. \tag{B.18}$$

As for the heating and cooling rates, normalizations factors are the same of course, and the only difference we have here is in the definition of the normalized rate functions for $H_\star$ and $H_{\rm Comp}$ (see Sect. 7), so that in the relativistic temperature regime, we define

$$h_\star(x) \;=\; \overline{C}_1 x^{\sigma_1} s^{2{\rm k_T}} (1+4\Theta)^{\rm k_T} + \overline{C}_2 x^{\sigma_2}, \tag{B.19}$$

$$l_{\rm Comp} \;=\; \left(\frac{\sigma_{\rm T} L_0}{2\pi m_{\rm e} c^2 \gamma c_{\rm sc} r_{\rm g}}\right) s^2 (1+4\Theta), \tag{B.20}$$

where $\Theta = s^2(3/10)(m_{\rm p}/m_{\rm e})(c_{\rm sc}/c)^2$. With the definitions above, and setting also

$$\overline{\mathcal{G}} - \overline{\mathcal{L}} \equiv h_*(1 - u c_{\rm sc}/c) + h_{\rm Comp} - l_{\rm Comp} - \frac{x_{\rm c}^2 f_{\rm m}}{u}\lambda, \tag{B.21}$$

normalized equations for relativistic electron temperature regime are the following:

$$\begin{aligned} u K_{\rm M} \frac{du}{dx} = {} & \\ & \frac{6s^2}{5x}\left(1+\frac{1}{f_{\rm T}}\right) - \frac{\overline{\mathcal{G}}-\overline{\mathcal{L}}}{u x^2 f_{\rm T}} + \frac{h_{\rm tot}}{x^2}\left(\frac{c_{\rm sc}}{c}\right) - \frac{1}{2x^2}\left(\frac{c}{c_{\rm sc}}\right)^2 \\ & - \frac{1}{f_{\rm m}}\frac{df_{\rm m}}{dx}\left[u^2\left(1+\frac{1}{2f_{\rm T}}\right) - \frac{3s^2}{5}\left(\frac{F}{f_{\rm T}}-1\right)\right], \end{aligned} \tag{B.22}$$

$$\begin{aligned} K_{\rm M}\frac{ds^2}{dx} = {} & \\ & -\frac{2s^2}{x f_{\rm T}} + \frac{5}{3}\frac{\overline{\mathcal{G}}-\overline{\mathcal{L}}}{u x^2 f_{\rm T}} P_{\rm M} - \frac{s^2 h_{\rm tot}}{x^2 u^2 f_{\rm T}}\left(\frac{c_{\rm sc}}{c}\right) + \frac{s^2}{2u^2 x^2 f_{\rm T}} \times \\ & \left(\frac{c}{c_{\rm sc}}\right)^2 + \frac{1}{f_{\rm m}}\frac{df_{\rm m}}{dx}\left[\frac{5}{6}\frac{u^2}{f_{\rm T}}\left(1 - \frac{6}{5}\frac{F s^2}{u^2}\right) P_{\rm M} \right. \\ & \left. + \frac{s^2}{f_{\rm T}}\left(1+\frac{3}{5}\frac{s^2}{u^2}\right)\right], \end{aligned} \tag{B.23}$$

where $M_{\rm r}$ and $P_{\rm M}$ are non-dimensional and, in terms of normalized quantities can be written explicitly as follows

$$M_{\rm r}^2 = \frac{5}{3}\frac{u^2}{s^2}\frac{1}{1+1/f_{\rm T}}, \qquad P_{\rm M} = K_{\rm M} + \frac{3}{5}\frac{s^2}{u^2 f_{\rm T}}. \tag{B.24}$$

References

Alexander T., Netzer H., 1994, MNRAS 270, 781
Alexander T., Netzer H., 1997, MNRAS 284, 967
Alexander T., 1997, MNRAS 285, 891
Begelman M.C., McKee C.F., Shields G.A., 1983, ApJ 271, 70
Begelman M.C., de Kool M., Sikora M., 1991, ApJ 382, 416
Birk G.T., Lesch H., Schopper R., et al., 1999, Astroparticle Physics 11, 63
Bittencourt J.A., 1988, Fundamentals of Plasma Physics. Pergamon Press, Oxford
Björnsson G., Svensson R., 1991, MNRAS 249, 177 (BS91)
Blandford R., 1993, In: Burgarella D., Livio M., O'Dea C.P. (eds.) Astrophysical Jets. Cambridge University Press, p. 15
Blandford R., 1994, In: Bicknell G.V., Dopita M., Quinn P.J. (eds.) The First Stromlo Symposium: The Physics of Active Galaxies. ASP, San Francisco, p. 23
Blandford R.D., Begelman M.C., 1999, MNRAS 303, L1
Chiang J., Murray N., 1996, ApJ 466, 704
Crenshaw D.M., Kraemer, 1999, ApJ 521, 572
Crenshaw D.M., Kraemer S.B., Boggess A., et al., 1999, ApJ 516, 750
David L.P., Durisen R.H., Cohn H.N., 1987, ApJ 313, 556
David L.P., Durisen R.H., 1989, ApJ 346, 618
de Kool M., 1997, In: Arav N., Shlosman I., Weymann R.J. (eds.) Mass Ejection from AGN. ASP Conference Series 128, ASP, San Francisco
Emmering R.T., Blandford R.D., Shlosman I., 1992, ApJ 385, 460
Esser R., et al., 1997, JGR 102, 7063
George I.M., Turner T.J., Netzer H., et al. 1998, ApJS 114, 73
Haardt F., Maraschi L., 1993, ApJ 413, 507
Haardt F., Maraschi L. Ghisellini G., 1994, ApJ 432, L95
Koratkar A., Blaes O., 1999, PASP 111, 1
Korista K., 1999, In: Ferland G., Baldwin J. (eds.) Quasars and Cosmology. ASP Conf. Series, ASP, San Francisco (astro-ph/9812043)
Krolik J.H., McKee C.F., Tarter C.B., 1981, ApJ 249, 422
Krolik J.H., Vrtilek J.M., 1984, ApJ 279, 521
Krolik J.H., Begelman M.C., 1986, ApJ 308, L55
Krolik J.H., 1988, ApJ 325, 148
Krolik J.H., 1999, Active Galactic Nuclei. Princeton University Press
Laing R.A., 1996, In: Eckers R., Fanti C., Padrielli L. (eds.) Extragalactic Radio Sources. IAU Symp. 175, Kluwer Academic Publishers, p. 147
Landau L.D., Lifshitz E.M., 1959, Fluid Mechanics. Pergamon Press, Oxford
Landini M., Monsignori Fossi B.C., 1990, A&AS 82, 229
Levich E.V., Syunyaev R.A., 1971, SvA; AJ 15, 363
Liang E.P.T., Price R.H., 1977, ApJ 218, 247
Mathews W.C., Ferland G.J., 1987, ApJ 323, 456
Mathews W.C., Doane J.S., 1990, ApJ 352, 423
Mathur S., Elvis M., Wilkes B., 1995, ApJ 452, 230
Mathur S., 1997, In: Arav N., Shlosman I., Weymann R.J. (eds.) Mass Ejection from AGN. ASP Conference Series 128, ASP, San Francisco, p. 161
Mathur S., Wilkes B.J., Aldcroft T., 1997, ApJ 478, 182
Mathur S., Elvis M., Wilkes B., 1999, ApJ 519, 605

Murray N., Chiang J., Grossman S.A., et al., 1995, ApJ 451, 498
Netzer H., Peterson B.M., 1997, In: Maoz D., Sternberg A., Leibovitz E. (eds.) Astronomical Time Series. Proceedings of the Wise Observatory 25^{th} Ann. Symp., Kluwer Academic Publishers, Dordrecht (astro-ph/9706039)
Raine D.J., O'Reilly M.D., 1993, Astro.Lett. and Communications 28, 331
Stocke J.T., Shull M.J., Granados A.F., et al., 1994, AJ 108, 1178
Torricelli-Ciamponi G., Pietrini P., 2000, in preparation
Turnshek D.A., 1988, In: Blades J.C., Turnshek D.A., Norman C.A. (eds.) QSO Absorption Lines. STScI Symp. 2, Cambridge Univ. Press, p. 17
Turnshek D.A., 1995, In: Meylan G. (ed.) QSO Absorption Lines. ESO Workshop Proc., Springer, p. 223
Ulrich M.-H., 1988, MNRAS 230, 121
Wandel A., 1998, In: Gaskell C.M., Brandt W.N., Dietrich M., et al. (eds.) Structure and Kinematics of Quasar Broad Line Region. ASP Conference, ASP, San Francisco (astro-ph/9808171)
Wandel A., Peterson B.M., Malkan M.A., 1999, ApJ 526, 579
Weymann R.J., Scott J.S., Schiano A.V.R., et al., 1982, ApJ 262, 497
Weymann R.J., Morris S.L., Gray M.E., et al., 1997, ApJ 483, 717
Zensus J.A., 1996, In: Eckers R., Fanti C., Padrielli L. (eds.) Extragalactic Radio Sources. IAU Symp. 175, Kluwer Academic Publishers, p. 5